NASA TECHNICAL NOTE

NASA TN D-3699

NASA TN D-3699

ANALYSIS OF USE OF JUPITER GRAVITY TURNS FOR TAILORING TRAJECTORIES TO SATURN WITH CONSIDERATION OF LAUNCH OPPORTUNITIES

by Edwin F. Harrison and Charles H. McLellan

Langley Research Center

Langley Station, Hampton, Va.

NATIONAL AERONAUTICS AND SPACE ADMINISTRATION • WASHINGTON, D. C. • NOVEMBER 1966

NASA TN D-3699

ANALYSIS OF USE OF JUPITER GRAVITY TURNS FOR TAILORING TRAJECTORIES TO SATURN WITH CONSIDERATION OF LAUNCH OPPORTUNITIES

By Edwin F. Harrison and Charles H. McLellan

Langley Research Center
Langley Station, Hampton, Va.

NATIONAL AERONAUTICS AND SPACE ADMINISTRATION

For sale by the Clearinghouse for Federal Scientific and Technical Information
Springfield, Virginia 22151 – Price $2.50

ANALYSIS OF USE OF JUPITER GRAVITY TURNS FOR TAILORING TRAJECTORIES TO SATURN WITH CONSIDERATION OF LAUNCH OPPORTUNITIES

By Edwin F. Harrison and Charles H. McLellan
Langley Research Center

SUMMARY

A trajectory study has been conducted to determine several launch opportunities for Earth to Saturn missions, especially those times when the intermediate planet Jupiter can be passed closely enough to use its strong gravitational field to make favorable, significant changes in the interplanetary-trajectory conditions. The effect of hyperbolic-excess velocity and flight-path angle at departure from Earth on both launch date and trip time are studied for the gravity-turn trajectories. These trajectory characteristics are compared with direct Earth to Saturn trajectory requirements. Passage distance, turning angle, and velocity gained at Jupiter for the gravity-assisted trajectories are examined. This study is based mainly on coplanar trajectories; however, an evaluation of noncoplanar effects is included.

Jupiter gravity turns can be utilized for missions to Saturn with launch dates in 1976, 1977, 1978, and 1979, and again starting in about 1996. With the approximate minimum-energy requirement for direct missions to Saturn, a reduction in trip time of about 40 percent was realized for the gravity-turn trajectories over the direct trajectories. By employing a gravity-turn mode, missions to Saturn can also be made with velocity levels at about 1 km/sec lower than the minimum value required for the direct trajectories. This reduction in required velocity can double the payload fraction for a fly-by Saturn mission if a launch vehicle with approximately the same capability as the Saturn V is used.

INTRODUCTION

As planetary exploration advances to more distant planets, the trip times become increasingly long and the energy requirements large. For example, a minimum-energy trajectory from Earth to Saturn requires about 6 years and a velocity of about 10.4 km/sec at departure from the Earth's sphere of influence. Shorter trip times can be obtained at the expense of an increased energy requirement, which, of course, is very costly in terms of payload fraction of the launch vehicle. Another approach that looks attractive for some

of these missions (refs. 1 and 2) is to utilize the free energy that can be derived from the gravitational field of the intermediate planet Jupiter when it is possible to pass near this planet before reaching Saturn. This gravitational effect is referred to in the literature as gravity turn, gravity assist, planet swingby, or planetary attraction. These studies of Earth-Jupiter-Saturn trajectories, as well as studies of Earth-Venus-Mars combinations (refs. 3, 4, and 5), have shown that the use of gravity-assisted trajectories can offer advantages, such as reductions in required launch velocity, trip time, or arrival velocity, when compared with the values for direct missions. If a huge planet like Jupiter can be used, its strong gravitational field can be very effective in tailoring interplanetary trajectories.

The use of a gravity turn at Jupiter for an Earth-Saturn mission requires particular combinations of the relative positions of all three planets; therefore, the number and frequency of the launch opportunities are limited. There has been very little consideration given to launch date in the literature[1] to disclose when full benefits from Jupiter gravity turns can be realized. However, one launch date for a specific launch velocity is discussed in reference 2.

The purpose of the present study is to determine, for Jupiter gravity-assisted trajectories to Saturn, launch dates for several launch opportunities and the corresponding trip times for a range of hyperbolic-excess velocities and to compare the results with direct-mission requirements. The passage distance, turning angle, and velocity gained at Jupiter for the gravity-assisted trajectories are also presented.

ANALYSIS

Coplanar Trajectories

A two-dimensional, two-body analysis was performed for the main part of the present study in order to determine approximate launch opportunities and the associated characteristics of Jupiter gravity-assisted trajectories to Saturn. In order to analyze the trajectories, they were divided into two main parts: (1) the departure from Earth to arrival at Jupiter and (2) the gravity turn and departure from Jupiter to arrival at Saturn. The geometry involved in these heliocentric trajectories is presented in figure 1. The planets are assumed to be point masses with their spheres of influence shrunk to zero for the heliocentric trajectories, and thus the trajectories go from the center of one planet to the center of another. However, for the gravity-turn maneuver at Jupiter, consideration must be given to the gravitational field of the planet and passage distance, as shown in figure 2.

[1]After submission of this report for publication, the authors learned of a similar, concurrent study by Jerry M. Deerwester entitled "Jupiter Swingby Missions to the Outer Planets," AIAA Paper No. 66-536, June 1966.

In general, the approach followed in this study is to simplify the analysis without seriously degrading its accuracy. Since the Earth-Jupiter central angles to be considered in this analysis will not be near 180°, the out-of-the-ecliptic inclination angles and velocity requirements are small and can be neglected for first-order approximations with good accuracy for mission feasibility studies; hence a coplanar trajectory can be used.

Since the eccentricity of Earth is very small, its orbit can be assumed to be circular with little error being introduced into the interplanetary trajectories. However, the eccentricities of Jupiter and Saturn are appreciable and must be accounted for.

The symbols used in the trajectory equations are defined in appendix A, and the equations used for the coplanar trajectories are given in appendix B. In order to evaluate the effect on the analysis of assuming that the trajectories are coplanar, some calculations were made for noncoplanar trajectories; the equations are presented in appendix C.

Earth to Jupiter trajectories.- The coplanar trajectory considered for this study begins at Earth, where the hyperbolic-excess velocity of the spacecraft and its heliocentric flight-path angle are specified. This velocity and angle are then used in the equations given in appendix B to calculate trajectories to Jupiter's elliptical orbit, where the arrival heliocentric radius depends on launch date and trip time. In order to determine the matching conditions between these trajectory parameters, a graphic iteration was employed. In this procedure, calculations of trip time, central angle, and heliocentric radius from the trajectory are uniquely matched with launch date and other comparable ephemeris data (refs. 6 and 7) of Earth and Jupiter. A detailed explanation of this matching procedure along with a graphic illustration is given in appendix B.

Jupiter to Saturn trajectories.- As the spacecraft passes Jupiter, the gravitational field of the planet causes changes in heliocentric direction and velocity, as schematically illustrated in figure 1. The change in the heliocentric velocity occurs because the arrival and departure hyperbolic-excess velocity vectors are different in direction but equal in magnitude. The spacecraft passes on the back side of the planet in an effort to increase the heliocentric velocity. The closest passage distance (see fig. 2) has to be determined such that the spacecraft is located on an encounter trajectory with Saturn, the target planet.

Because of the number of variables involved, both calculations and graphs are used to determine the proper passage distance at Jupiter. Trajectories are computed from the equations in appendix B by using the determined arrival conditions and various selected values for the passage distance and the heliocentric radius to Saturn. These trajectory calculations are then plotted along with Jupiter and Saturn ephemeris data, and matched conditions are obtained. (See appendix B.) The matched trajectory conditions include: trip time, central angle, heliocentric radius, and passage distance. With these quantities

determined, the desired coplanar trajectory to Saturn involving a gravity assist at Jupiter is established.

It should be noted that this two-dimensional analysis provides only approximate conditions for the gravity-assisted trajectories. For the purpose of determining the accuracy of this analysis a noncoplanar or a simplified three-dimensional analysis was also performed.

Noncoplanar Trajectories

When the orbital inclination of Jupiter is taken into account, the orbital plane of the spacecraft, which is assumed to lie in the ecliptic for the two-dimensional analysis, has to be changed in order to intercept Jupiter. This orbital plane change requires additional velocity, which is considered for convenience to be applied either at Earth upon departure or at Jupiter's ascending node. At either location, all the coplanar characteristics between Earth and Jupiter, except of course the total velocity requirement, can be maintained by rotating the velocity vector of the spacecraft coplanar trajectory in a plane normal to the elliptic. These plane changes are shown graphically in figure 3 and the equations are presented in appendix C.

If the orbital plane of the spacecraft is inclined to the ecliptic upon departure from Earth, then it will intercept Jupiter's orbital plane upon arrival at the angle of declination $i_{2,J}$. (See fig. 4.) Hence, the equations for the coplanar trajectory become inapplicable at Jupiter and for the Jupiter to Saturn phase of the mission. Equations were developed (see appendix C) to allow for the angles between the approach and departure planes of the spacecraft at Jupiter. Noncoplanar trajectories were then calculated from these equations and matched with planetary ephemeris data, in a manner similar to that used for the coplanar trajectory between Jupiter and Saturn.

RESULTS AND DISCUSSION

General Effects of Gravity Turns

Before considering specific launch opportunities and trajectories, some of the general characteristics of the Jupiter gravity-turn mode for circular planetary orbits are examined. The closest passage distance of the spacecraft at Jupiter is one of the prime factors because it has a strong effect on the Jovian departure flight-path angle, which results in heliocentric velocity gains, as shown in figures 5 and 6. For each value of the Earth departure hyperbolic-excess velocity $V_{h,1}$ considered, the maximum heliocentric velocity gained at Jupiter occurs when the spacecraft passes near the surface of the planet. This spacecraft position corresponds to a Jovian departure flight-path angle of 0°. It might be first thought that these conditions would yield the minimum trip time to Saturn.

However, the data in figure 7 show that the minimum trip times usually occur when the passage distance is several radii from the planet, where the velocity gained is less than the maximum possible value. Thus, as the passage distance increases to some extent, the associated change in Jovian departure flight-path angle can more than compensate for the decrease in velocity gained.

A comparison of the minimum trip times in figure 7 with direct trip times is presented in figure 8. A large reduction in trip time for a specified value of $V_{h,1}$ or a decrease in the required value of $V_{h,1}$ for a selected trip time is shown for the gravity-turn trajectory as compared with the direct trajectory. In order to use such gravity turns, however, the ephemeris of the planets must be considered and launch opportunities determined.

Position Requirements of Planets

The relative positions of the planets for a 30-year period and the approximate angle requirements of them at launch time for the Jupiter gravity-turn trajectories are shown in figure 9. The ephemeris angles presented are the differences in the heliocentric longitudes of Jupiter and Earth along with the corresponding differences in the positions of Jupiter and Saturn. (See refs. 6 and 7.) The Earth-Jupiter synodical cycle is about 1 year, whereas the Jupiter-Saturn synodical period is nearly 20 years. The relative locations of the planets required for the gravity-turn trajectories were determined as follows:

Trajectory transfer angles were calculated for Earth departure hyperbolic-excess velocities ranging from 10.363 km/sec (34 000 fps), representing the approximate minimum-velocity requirements for a direct trajectory to Saturn, to an arbitrary value of 12.192 km/sec (40 000 fps); the departure heliocentric flight-path angle at Earth was initially 0°. These computed angles were then transferred, by using the motion of planets, to the angles required between the planets at launch. The shaded areas in figure 9 represent the required angles. When the ephemeris data lines for the planets pass through the required-angle regions for the trajectories, launch opportunities become available. The Jupiter-Sun-Earth angle requirement can be met almost every year; however, there is only about a 3-year period every 20 years in which the required and available Saturn-Sun-Jupiter angles can be matched. From this figure it can be seen, therefore, that launch opportunities for Jupiter gravity-assisted trajectories will be available in 1976, 1977, 1978, and 1979, and again starting in 1996 for the velocities considered.

Effects of Hyperbolic-Excess Velocity on Trajectory Characteristics

For the 1978 launch opportunity, the effect of the hyperbolic-excess velocity on other trajectory characteristics such as launch window, turning angle and closest passage distance at Jupiter, heliocentric profiles, and trip times for Jupiter gravity trajectories to Saturn are presented in figures 10 to 12. These results are based on the coplanar trajectory analysis.

The data of figure 10 show that the range of hyperbolic-excess velocities considered for tangential launches from Earth's orbit provides a launch window of about 8 days in 1978 for both Jupiter gravity-turn and comparable direct trajectories to Saturn. Although only one launch date is shown to be available for a given value of $V_{h,1}$ because $\gamma_1 = 0^o$, the launch window can be enlarged by varying γ_1. For the present launch conditions, the corresponding Earth-Saturn trip times are shown in the upper part of this figure. A variation of the hyperbolic-excess velocity at Earth was shown to have the greatest effect on trip time at the lower velocities. At the approximate minimum velocity for a direct mission, the trip time obtained for the gravity-turn trajectory is as much as 40 percent lower than that for the direct trajectory. When both types of trajectories have the same trip time, say 5 years, an important reduction of about 1 km/sec or approximately 10 percent in hyperbolic-excess velocity is indicated for the gravity-turn trajectory. Also presented in figure 10 is the injection velocity, which is equal to the square root of the sum of squares of the hyperbolic-excess velocity and the escape velocity. Thus, the 10-percent reduction in hyperbolic-excess velocity corresponds to lowering the injection velocity by about 5 percent.

Another possible use of the gravity turn is to provide additional launch windows, which would be approximately a month ahead of the direct-mission launches. For example, if a value of 11 km/sec can be attained for $V_{h,1}$, it would be possible, in 1978, to launch on October 10 by using a gravity-turn trajectory or on November 5 by using a direct trajectory to Saturn. (A shift of a few days in these launch dates will, of course, occur when an exact analysis is used.)

The closest passage distance and turning angle which correspond to the trajectory characteristics of figure 10 are presented in figure 11. The hyperbolic-excess velocity is shown to have a pronounced effect on the passage distance required at Jupiter. This effect was strongest at the lower velocities where a decrease of 1 km/sec caused an increase in the passage distance of about 30 Jupiter radii, while the corresponding turning angle decreased only about 8^o.

Illustrated in figure 12 is the effect of the hyperbolic-excess velocity on the heliocentric profile of the gravity-turn trajectory from Earth to Saturn. No appreciable effects

on the appearance of the trajectories are evident, even though there is nearly a year difference in the trip times.

Comparison of Coplanar and Noncoplanar Trajectories

All the preceding results are based on coplanar trajectories determined from a two-dimensional analysis. In table I, a comparison is made of some of the results obtained from this analysis with those determined by a similar analysis in reference 2 for a particular launch. The present data agree well with reference results. The small difference in them can generally be contributed to the difference in heliocentric radii used.

In order to determine the uncertainties involved in the results of the coplanar trajectories, they are compared with noncoplanar results in table II. The coplanar results are in good agreement with those of the noncoplanar trajectories; therefore, the coplanar results presented in this report can be relied on to represent good approximations and proper trends for mission planning. A comparison is not made of the present results with the Earth-Jupiter-Saturn trajectory results given in reference 8, because a 30° error was made in determining the heliocentric position of Saturn in that report, as noted in reference 9.

Whereas the departure velocity from the Earth's orbit is assumed to be the same for the coplanar and noncoplanar trajectories, a velocity increment is required to change the trajectory plane so that the trajectory will intercept Jupiter. As discussed in appendix C, this velocity increment can be added in such a way that the plane change is obtained without a change in the heliocentric velocity or the flight-path angle of the spacecraft. For convenience, the plane change is considered to occur either at the departure from Earth or at Jupiter's node. In figure 13, the additional velocity required for these plane changes is presented as a function of launch date for a given hyperbolic-excess velocity. For the gravity-turn trajectories, the additional velocity required is very small when it is applied at departure from Earth, because here it can be combined with the coplanar hyperbolic-excess velocity and used as a single impulsive velocity. At Jupiter's node the velocity increment shown represents the total propulsion required there. Regardless of the plane-change location, the comparable direct trajectories shown require a larger velocity increment than the gravity-turn trajectories, mainly because they have transfer angles of almost 180°. However, none of the velocity increments given in figure 13 are included in the other results presented in this report, because they can be included after the trajectories are determined.

Both the angular approach and the departure inclination angle at Jupiter affect the Jupiter-Saturn leg of the gravity-turn trajectory. The approach characteristics depend on the location of the spacecraft when the plane change is initiated before reaching Jupiter. Because of the small velocity increment required for a plane change at departure from

Earth for the gravity-turn trajectories (see fig. 13), this location was used for the noncoplanar trajectories. The required values of the parameters at departure, however, can be attained without propulsive velocity by making proper use of the gravity-turn maneuver, even when Saturn's orbital inclination is included. For example, an upward deflection of the departure velocity can be obtained by approaching Jupiter below its orbital plane.

Effects of Launch Year on Trajectory Characteristics

As indicated in figure 9, launch opportunities for gravity-assisted trajectories to Saturn will be available in 1976, 1977, 1978, 1979, and again in about 20 years. The effect of these opportunities on trip time is presented in figure 14 along with comparable direct trip times required for the same hyperbolic-excess velocity. For these launches with $V_{h,1}$ of 10.363 km/sec, the trip time for any particular gravity-turn trajectory is some 35 to 45 percent less than that of the direct trajectory. The shortest trip times for the gravity-turn trajectories are in 1977 and 1978. Also, there is good agreement between the trip times of the coplanar and the noncoplanar trajectories.

The corresponding passage distance and turning angle at Jupiter required for the gravity-assisted trajectories shown in figure 14 are a strong function of launch year, as illustrated in figure 15. The closest passage distance occurs for the 1976 launch date; for each succeeding launch date, the passage distance increases very rapidly. No launch opportunities in which the gravity turn could be used were found prior to 1976, even though a range of values of $V_{h,1}$ were considered. For the 1979 launch date shown in figure 15, the passage distance is over 100 Jupiter radii and the turning angle is only about 10°. These results indicate that for launches later than 1979 there probably would be only small advantages gained (i.e., reduced trip time) by using a gravity turn, unless the hyperbolic-excess velocity at Earth is increased. (See fig. 11.) The turning angle and passage distance for the coplanar trajectories shown in figure 15 agree reasonably well with those of the noncoplanar trajectories, except for the passage distance at the 1979 launch date. For this date, the passage distance is so far from the planet that its effect on the trajectory would be rather small anyway.

Presented in figure 16 are the actual velocity gained and the angle change at Jupiter associated with the launches from 1976 to 1979. These trajectory changes are strongly influenced by the passage distance, and their maximum values are obtained for the 1976 launch date, which had the closest passage distance to Jupiter (fig. 15). For this launch date the magnitudes of these parameters are large: about 11.5 km/sec is gained in spacecraft velocity and a change of approximately 63° occurs in the flight-path angle. For this trajectory almost maximum utilization is made of this free velocity which is available at Jupiter. (See fig. 5.)

As the velocity gained at Jupiter increases, the arrival hyperbolic-excess velocity at Saturn becomes larger as shown in figure 17. A comparison of these arrival velocities with those of direct trajectories for comparable trip times has not been made here. However, such a comparison has been made in reference 10 and, although the details are not shown, the comparison indicates that arrival velocities are so high that if an orbiter mission to Saturn is desired, the Jupiter gravity turns become less attractive than the direct missions.

In figure 18, heliocentric profiles of the spacecraft trajectory for the launches from 1976 to 1979 for Earth-Jupiter-Saturn missions are presented. The Earth-Jupiter central angles of the trajectories have essentially the same value for all the launches, even though they start at different points. However, the Jupiter-Saturn central angle decreases considerably for each succeeding launch year because the trip time remains about the same (fig. 14), while the gain in velocity and the flight-path angle change at Jupiter (fig. 16) decrease.

Solar Occultation

As the spacecraft approaches Saturn, the line of sight to Earth can possibly be occulted by the Sun. The effect of trip time on this solar occultation is presented in figure 19. The trip time should be something other than about 3.1 years for the launch conditions considered in order to avoid solar occultation. In order to insure a clear line of sight, the Saturn-Sun-Earth angle should probably be less than about 170° because of the extension of the Sun's corona.

Variation of Flight-Path Angle

All the preceding results have been for a tangential launch (i.e., $\gamma_1 = 0^{\circ}$), and thus the launch window is very narrow for a particular year. In order to widen this launch window, the departure flight-path angle at Earth was varied for a constant hyperbolic-excess velocity. The results for the gravity-assisted trajectories are shown in figure 20. A variation from -4° to 4° in the flight-path angle produced a launch window of about 15 to 20 days, depending on the launch year. This extension of the launch window should provide enough time for launch considerations.

The effect of flight-path angle at Earth on trip time is presented in figure 21. Even though the hyperbolic-excess velocity was held constant, the departure heliocentric velocity at Earth of the spacecraft decreased as the flight-path angle changed. Therefore, the trip time increased as the flight-path angle varied from 0°. As pointed out earlier, the minimum trip times are for the launches in 1977 and 1978.

The combination effect of hyperbolic-excess velocity and flight-path angle on the launch window is illustrated in figure 22 for the launch year 1978. As the flight-path angle varies from -4° to 4°, the number of available days for launch is shown to be about 19 and

is almost independent of the hyperbolic-excess velocity considered. For a particular flight-path angle, the launch date is moved forward only about 3.5 days for a 1 km/sec increase in velocity.

Figure 23 shows the effect of hyperbolic-excess velocity and flight-path angle on trip time. As expected, the shortest trip times occur when the hyperbolic-excess velocity increases and the flight-path angle approaches 0^{o}.

Payload Comparison

A comparison of the payload fraction for a direct mission with that for a Jupiter gravity-turn mission to Saturn is presented in figure 24. The line shown represents the capability of a launch vehicle which is approximately the same as that of a Saturn V. The circular- and square-shape symbols on this line represent the minimum velocity requirements for a Jupiter gravity-turn and a direct trajectory to Saturn, respectively, for a typical launch opportunity. These results indicate that a payload fraction for a fly-by Saturn mission can be doubled by employing a Jupiter gravity-turn trajectory. Furthermore, the trip time would be shorter for the gravity-turn trajectory, according to figure 10.

Other Considerations

This study has been concerned with only pure gravity turns at Jupiter, which have been demonstrated to be very advantageous for Earth to Saturn trajectories. However, more improvement in the performance characteristics of these trajectories might be obtained in future studies if the gravity turn is augmented with propulsion. In reference 11, Mars nonstop round-trip trajectories with gravity and propulsion gravity turns are analyzed. Compared with gravity turns, propulsion-augmented gravity turns near Mars markedly expanded the range of possible trip times and favorable launch dates and, in some cases, reduced the required total propulsion velocity increment.

Another aspect of the Jupiter gravity-turn trajectory that appears to need future consideration is the guidance and communication requirement for these missions. One study (ref. 12) has been made for an Earth-Venus-Mercury mission, and no areas of serious difficulties with regard to tracking, communication, or guidance were found. The results, however, indicated that combinations of some of the other planets would be more sensitive to errors in guidance.

CONCLUDING REMARKS

A two-dimensional analysis has been conducted on the utilization of the gravitational field of Jupiter for tailoring trajectories to Saturn. For these missions, launch dates in

1976, 1977, 1978, and 1979 have been determined for a value of the departure hyperbolic-excess velocity at Earth of near the minimum value required for a direct mission to Saturn. A reduction in the Earth-Saturn trip time of approximately 40 percent was realized for these gravity-assisted trajectories over the direct trajectories. The closest passage distance to Jupiter varied from very near the surface of the planet to more than 100 Jupiter radii as the launch opportunity advanced from 1976 to 1979.

For the gravity-turn analyses, the results obtained from the coplanar-trajectory equations agreed well with the noncoplanar values.

A variation of the hyperbolic-excess velocity at Earth was shown to have the greatest effect on trip time at the lower velocities. Gravity-assisted trajectories to Saturn can actually be made with values of the hyperbolic-excess velocity which are a significant 10 percent lower than the minimum velocity required for a direct trajectory. This reduction in required velocity can double the payload fraction for a fly-by Saturn mission if a launch vehicle having approximately the same capability as a Saturn V is used.

Langley Research Center,
National Aeronautics and Space Administration,
Langley Station, Hampton, Va., June 22, 1966.

APPENDIX A

SYMBOLS

a	semimajor axis, kilometers
E	eccentric anomaly, radians
e	eccentricity
F	hyperbolic anomaly, radians
I_{sp}	specific impulse, meters/second
$i_{J,E}$	orbital inclination of Jupiter to ecliptic, degrees
$i_{1,E}$	inclination angle between orbital planes of spacecraft and Earth at departure, degrees
$i_{2,J}$	declination angle between orbital planes of spacecraft and Jupiter at Jovian arrival, degrees
$i_{3,J}$	inclination angle between orbital planes of spacecraft and Jupiter at Jovian departure, degrees
l	heliocentric longitude of planet, degrees
$l_{E,1}$	heliocentric longitude of Earth at time of departure from it, degrees
$l_{J,3}$	heliocentric longitude of Jupiter at time of departure from it, degrees
Q	velocity vector connecting arrival with departure hyperbolic-excess velocity vectors at Jupiter (see fig. 4), kilometers/second
R_J	radius of Jupiter, kilometers
R_P	periapsis distance of spacecraft from center of Jupiter, kilometers
r	radial distance of body from center of Sun, kilometers

r_a	apoapsis distance, kilometers
r_p	periapsis distance, kilometers
T	date with respect to orbital position of planet, Julian date
$T_{E,1}$	date at departure from Earth, Julian date
$T_{J,3}$	date at departure from Jupiter, Julian date
t	time from periapsis, years
$t_{1,2}$	trip time from Earth to Jupiter, years
$t_{3,4}$	trip time from Jupiter to Saturn, years
V	velocity of body relative to Sun, kilometers/second
V_c	circular velocity of Jupiter at surface of planet, kilometers/second
V_h	hyperbolic-excess velocity relative to planet, kilometers/second
$\Delta V_{h,1}$	velocity increment required to be combined with coplanar hyperbolic excess at Earth to make a plane change, kilometers/second
V_n	velocity of spacecraft at Jupiter's node, kilometers/second
ΔV_n	velocity increment required at Jupiter's node to make a plane change, kilometers/second
X	axis which lies along intersection of orbital planes of spacecraft and Jupiter (see fig. 4)
x	direction of vernal equinox
Y	axis which is perpendicular to X-axis and lies in Jupiter's orbital plane
Z	axis which is perpendicular to Jupiter's orbital plane

z	distance out of ecliptic, kilometers
z'	distance between planes of Jupiter and Saturn upon arrival at Saturn, kilometers
α	gravity-turn angle with respect to Jupiter, degrees
β	angle between hyperbolic-excess velocity vector of spacecraft and orbital velocity vector of planet, degrees
γ	flight-path angle relative to local normal of heliocentric radius vector, degrees
γ_n	flight-path angle of spacecraft at Jupiter's node, degrees
θ	orbital central angle measured from periapsis, degrees
$\theta_{1,2}$	Earth-Jupiter central angle, degrees
$\theta_{3,4}$	Jupiter-Saturn central angle, degrees
$\dot{\theta}_{1,n}$	central angle between Earth at departure and ascending node of Jupiter, degrees
μ	gravitational constant of Sun, kilometers^3/second^2
ξ_J	celestial latitude of Jupiter at arrival, degrees
σ	ratio of structural weight to booster stage weight
ψ	angle between hyperbolic-excess velocity vector of spacecraft and Jupiter's plane, degrees
Ω	longitude of ascending node, degrees

Subscripts:

1	trajectory conditions of spacecraft at departure from Earth
2	trajectory conditions of spacecraft at arrival at Jupiter

3	trajectory conditions of spacecraft at departure from Jupiter
4	trajectory conditions of spacecraft at arrival at Saturn
E	Earth's orbital conditions
J	Jupiter's orbital conditions
S	Saturn's orbital conditions

APPENDIX B

EQUATIONS USED FOR THE COPLANAR TRAJECTORIES

The type of coplanar trajectory considered in this paper may be divided into two parts: (1) the departure from Earth to arrival at Jupiter and (2) the gravity turn and departure from Jupiter to arrival at Saturn. Most of the equations required to define the characteristics of this trajectory have been developed (ref. 13) or depend only on simple geometric laws; hence, they will be presented herein with a minimum of description.

Earth to Jupiter Trajectories

The spacecraft is assumed to depart from Earth on an interplanetary trajectory to Jupiter (fig. 1) with a specified hyperbolic-excess velocity $V_{h,1}$ and flight-path angle γ_1. The radial distance from the Sun at the departure point r_1 is assumed to be 1.49×10^8 km, but the elliptical heliocentric radius of Jupiter r_2 is a variable. By employing all these conditions, trajectories can be computed from the following equations. These equations are arranged in the order required for a straightforward, step-by-step calculation procedure.

The departure heliocentric velocity at Earth, based on the geometry in figure 1 and the laws of cosines and sines, is

$$V_1^2 = V_E^2 + V_{h,1}^2 - 2V_E V_{h,1} \cos \beta_1 \tag{B1}$$

where

$$V_E^2 = \frac{\mu}{r_1}$$

$$\beta_1 = 180 - \gamma_1 - \sin^{-1}\left(\frac{V_E}{V_{h,1}} \sin \gamma_1\right)$$

The next seven equations are some of the fundamental elliptic orbit element relations as given in reference 13.

Semimajor axis:

$$a = \frac{r_1}{2 - \frac{r_1 V_1^2}{\mu}} \tag{B2}$$

Eccentricity:

$$e^2 = 1 - \frac{r_1}{a^2}(2a - r_1) \cos^2 \gamma_1 \tag{B3}$$

APPENDIX B

Perisapsis distance:

$$r_p = a(1 - e) \tag{B4}$$

Apoapsis distance:

$$r_a = a(1 + e) \tag{B5}$$

Orbital central angle:

$$\theta = \cos^{-1}\left(\frac{a - ae^2 - r}{er}\right) \tag{B6}$$

Eccentricity anomaly:

$$E = \cos^{-1}\left(\frac{a - r}{ae}\right) \tag{B7}$$

Time from periapsis:

$$t = \sqrt{\frac{a^3}{\mu}}\,(E - e \sin E) \tag{B8}$$

The following two equations are employed to transfer the reference point from the periapsis for the central angle and travel time to the departure point at Earth:

Earth-Jupiter central angle:

$$\theta_{1,2} = \theta_2 \pm \theta_1 \qquad \left(\pm\theta_1 \text{ for } \mp\gamma_1\right) \tag{B9}$$

Earth-Jupiter trip time:

$$t_{1,2} = t_2 \pm t_1 \qquad \left(\pm t_1 \text{ for } \mp\gamma_1\right) \tag{B10}$$

It should be noted that θ_1 and t_1 are determined by using $r = r_1 = 1.49 \times 10^8$ km and θ_2 and t_2 are determined by using $r = r_2$ in equations (B6) and (B8).

In order to determine the launch date and the corresponding trip time to Jupiter for the particular trajectory considered (i.e., the values of $V_{h,1}$ and γ_1 are specified) the calculated results from equations (B9) and (B10) are plotted in sketch (a) along with some planetary ephemeris data taken from references 6 and 7. The resultant angle $l_J - l_{E,1}$ is the difference between the heliocentric ecliptic longitude of Jupiter after some period of

time from a selected Earth departure date and that of Earth at the departure date. The time $T - T_{E,1}$ is the elapsed time after the Earth departure date, and the corresponding heliocentric radius to Jupiter is r_J.

The point where the curve for the calculated trajectories intercepts the same departure date line in both parts of sketch (a) determines the matching conditions of the Earth to Jupiter phase of the desired trajectory. It should be noted that the spacecraft will not actually intercept Jupiter, but the orbit of the planet is a convenient boundary point for the first part of the heliocentric trajectory calculations.

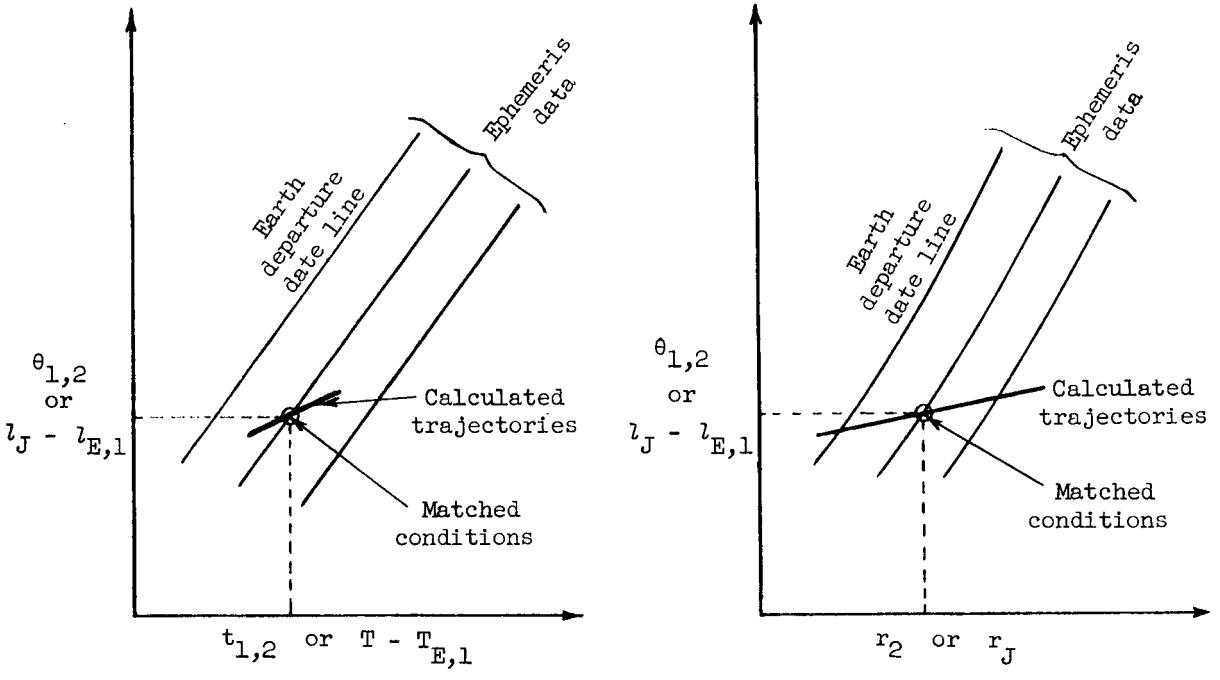

Sketch (a)

Other matching conditions at arrival at Jupiter can be determined by using the matched value of r_2 from the right-hand side of sketch (a) in the next four equations, which come either from reference 13 or the law of cosines.

Arrival flight-path angle:

$$\gamma_2 = \cos^{-1}\sqrt{\frac{r_a r_p}{r_2(r_a + r_p - r_2)}} \tag{B11}$$

APPENDIX B

• Arrival heliocentric velocity:

$$V_2^2 = \left(2 - \frac{r_2}{a}\right)V_J^2 \tag{B12}$$

where $V_J^2 = \frac{\mu}{r_2}$. (B13)

Arrival hyperbolic-excess velocity:

$$V_{h,2}^2 = V_J^2 + V_2^2 - 2V_J V_2 \cos \gamma_2 \tag{B14}$$

Jupiter to Saturn Trajectories

Upon arrival at Jupiter, the gravitational field of the planet causes a perturbation in the spacecraft trajectory. (See fig. 1.) This perturbation is a strong function of the closest passage distance (fig. 2), the value of which must be such that the departing spacecraft will lie on an intercept trajectory with Saturn.

The method employed in determining the closest passage distance is somewhat similar to that used for the Earth to Jupiter transfer. A number of trajectories are calculated by using the following equations ((B15) to (B29)) with the previously determined arrival conditions; the passage distance R_P and the heliocentric radius of Saturn r_4 are considered as variables. The actual matching procedure used is given after the equations.

The gravity-turn angle with respect to Jupiter, as shown in figure 2 and derived in reference 14, is:

$$\alpha = 2 \sin^{-1}\left[\frac{1}{\left(\frac{R_P}{R_J}\right)\left(\frac{V_{h,2}}{V_c}\right)^2 + 1}\right] \tag{B15}$$

where $V_c = 42.581$ km/sec for Jupiter.

For pure gravity turns,

$$V_{h,2} = V_{h,3} \tag{B16}$$

because no propulsive velocity is added.

APPENDIX B

The law of cosines can be applied to determine the departure heliocentric velocity and the flight-path angle at Jupiter. The resultant departure heliocentric velocity at Jupiter is:

$$V_3^2 = V_J^2 + V_{h,3}^2 - 2V_J V_{h,3} \cos(\beta_2 + \alpha) \tag{B17}$$

$$\left(\frac{V_3}{V_J}\right)^2 = 1 + \left(\frac{V_{h,3}}{V_J}\right)^2 - 2\frac{V_{h,3}}{V_J} \cos(\beta_2 + \alpha) \tag{B17a}$$

where

$$\beta_2 = \cos^{-1}\left(\frac{V_J^2 + V_{h,2}^2 - V_2^2}{2V_J V_{h,2}}\right)$$

and the departure flight-path angle is

$$\gamma_3 = \cos^{-1}\left(\frac{V_J^2 + V_3^2 - V_{h,3}^2}{2V_J V_3}\right) \tag{B18}$$

If in equation (B17a), $\left(\frac{V_3}{V_J}\right)^2 < 2$, elliptical equations (B19) to (B22) should be used, and if $\left(\frac{V_3}{V_J}\right)^2 > 2$, hyperbolic equations (B23) to (B29) should be used. In the elliptical and hyperbolic relationships which follow, the matching value of r_2 determined in the right-hand side of sketch (a) is used for r_3.

The following elliptical equations are obtained from reference 13:

Semimajor axis:

$$a = \frac{r_3}{2 - \frac{r_3 V_3^2}{\mu}} \tag{B19}$$

Eccentricity:

$$e^2 = 1 - \frac{r_3}{a^2}(2a - r_3)\cos^2\gamma_3 \tag{B20}$$

For the orbital central angle, eccentric anomaly, and time from periapsis passage, the general elliptical equations (B6), (B7), and (B8) are applicable and thus are employed. The reference axis of these equations can then be transferred to the departure point at Jupiter. The Jupiter-Saturn central angle, obtained by adding or subtracting the central angle between the periapsis and the departure point at Jupiter θ_3 to or from the central angle between the periapsis and the arrival point at Saturn, θ_4 is:

$$\theta_{3,4} = \theta_4 \pm \theta_3 \qquad \left(\pm\theta_3 \text{ for } \mp\gamma_3\right) \tag{B21}$$

Similarly, the Jupiter to Saturn trip time is

$$t_{3,4} = t_4 \pm t_3 \qquad \left(\pm t_3 \text{ for } \mp\gamma_3\right) \tag{B22}$$

The following hyperbolic equations are obtained from reference 13:

Semimajor axis:

$$a = \frac{r_3}{\frac{r_3 V_3^2}{\mu} - 2} \tag{B23}$$

Eccentricity:

$$e^2 = 1 + \frac{r_3}{a^2}(2a + r_3)\cos^2\gamma_3 \tag{B24}$$

Orbital central angle:

$$\theta = \cos^{-1}\left(\frac{-a + ae^2 - r}{er}\right) \tag{B25}$$

Hyperbolic anomaly:

$$F = \cosh^{-1}\left(\frac{a + r}{ae}\right) \tag{B26}$$

Time from periapsis:

$$T = \sqrt{\frac{a_3}{\mu}}(-F + e \sinh F) \tag{B27}$$

As was done for the elliptical transfers, the reference point of the central angle and the time of the hyperbolic trajectories between Jupiter and Saturn is transferred to the departure point at Jupiter from the periapsis. Thus the Jupiter-Saturn central angle is:

$$\theta_{3,4} = \theta_4 \pm \theta_3 \qquad \left(\pm\theta_3 \text{ for } \mp\gamma_3\right) \tag{B28}$$

and the Jupiter-Saturn trip time becomes

$$t_{3,4} = t_4 \pm t_3 \qquad \left(\pm t_3 \text{ for } \mp\gamma_3\right) \tag{B29}$$

In order to determine the matching trajectory-planetary conditions between Jupiter and Saturn, the results from equations (B21) and (B22) or (B28) and (B29) and the ephemeris data (refs. 6 and 7) are plotted as shown in sketch (b). In this sketch the resultant angle $l_S - l_{J,3}$ represents the difference between the heliocentric ecliptic longitude of Saturn after the known departure date from Jupiter and that of Jupiter at the time of departure. The time $T - T_{J,3}$ is the elapsed time after the Jupiter departure date, and r_3 is the corresponding radius to Saturn.

The points in the right-hand plot of sketch (b) where the curves for the calculated trajectories cross the Jupiter departure date line determine the values of $\theta_{3,4}$ that are used in the left-hand plot of sketch (b) to form a line between the trajectories. The point where this line and the departure date line intersect in the left-hand plot determines the

matching conditions for $\theta_{3,4}$ and $t_{3,4}$ for the trajectory considered. Then the line connecting the trajectories is replotted so that the passage distance can be obtained directly for matching conditions. This procedure completes the determination of all the matching conditions of the Jupiter-Saturn phase of the desired trajectory. Now all conditions have been established for a coplanar trajectory going from Earth to close passage of Jupiter and continuing on to Saturn.

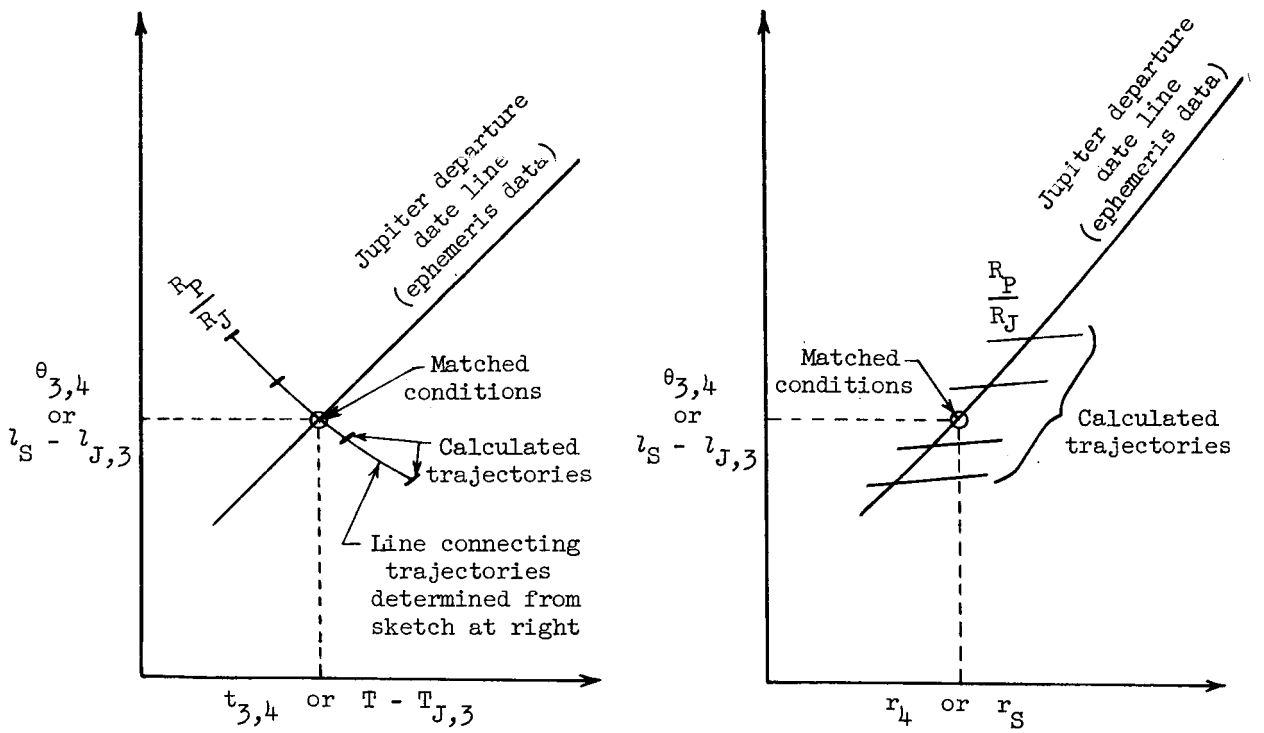

Sketch (b)

APPENDIX C

EQUATIONS USED FOR THE NONCOPLANAR TRAJECTORIES

Location of Plane Changes

Additional velocity is required for the coplanar trajectories when the orbital inclination angle of Jupiter is included. The point of application of this velocity may be considered to be either at Earth upon departure or at Jupiter's ascending node. In either case, all the matched characteristics from equations (B1) to (B12) for the coplanar trajectories between Earth and Jupiter can be maintained by rotating the velocity vector in a plane normal to the ecliptic. The geometry used to describe these plane-change maneuvers is presented in figure 3.

Plane change at Earth.- The inclination angle $i_{1,E}$ required for a plane change at Earth can be related to the Earth-Jupiter central angle $\theta_{1,2}$ and the celestial latitude ξ_J of Jupiter at arrival:

$$i_{1,E} = \sin^{-1}\left(\frac{\sin \xi_J}{\sin \theta_{1,2}}\right) \tag{C1}$$

If the heliocentric velocity V_1 is held constant, the velocity increment that must be added to the coplanar hyperbolic-excess velocity at Earth for a plane change is

$$\Delta V_{h,1} = \sqrt{V_1^2 + V_E^2 - 2V_1 V_E \cos i_{1,E}} - V_{h,1} \tag{C2}$$

where

$$V_1 = V_E + V_{h,1}$$

and

$$\gamma_1 = 0$$

Plane change at Jupiter's node.- Even when it is desirable to wait until the spacecraft reaches Jupiter's ascending node to make a plane change, the trajectory characteristics such as semimajor axis a, eccentricity e, and launch date are the same as for the coplanar trajectory. The central angle between Earth and the ascending node of Jupiter is

$$\theta_{1,n} = \Omega_J \pm l_{E,1} \tag{C3}$$

where Ω_J is the longitude of Jupiter's ascending node and $l_{E,1}$ is the longitude of Earth at departure. (See fig. 3(b).) The velocity of the spacecraft at the node is

$$V_n = \sqrt{\frac{2\mu(1 + e \cos \theta_{1,n})}{a(1 - e^2)} - \frac{\mu}{a}} \tag{C4}$$

This velocity must be rotated through an angle equal to the orbital inclination of Jupiter $i_{J,E} = 1.306^{\circ}$. The rotation of the velocity vector requires a velocity increment

$$\Delta V_n = 2V_n \cos \gamma_n \sin\left(\frac{i_{J,E}}{2}\right) \tag{C5}$$

where γ_n is the flight-path angle of the spacecraft at the node.

Jupiter to Saturn Trajectories

As stated earlier, up to the time of arrival at Jupiter, equations (B1) to (B12) are applicable for the noncoplanar trajectories. However, equations (B13), (B14), (B17), and (B18) are not applicable when the inclination angle from equation (C1) is included. Therefore, instead of assuming a 0° arrival declination angle, it can be included and determined from:

$$i_{2,J} = \sin^{-1}\left(\sin i_{J,E} \sqrt{\frac{r_J^2 - \frac{z_J^2}{\sin i_{J,E}^2}}{r_J^2 - z_J^2}}\right) + \sin^{-1}\left(\sin i_{1,E} \sqrt{\frac{r_J^2 - \frac{z_J^2}{\sin i_{1,E}^2}}{r_J^2 - z_J^2}}\right) \tag{C6}$$

This expression is based on the geometry presented in figures 3 and 4 and the out-of-ecliptic characteristics of Jupiter.

If this declination angle and all the elements of Jupiter's elliptical orbit are taken into account, the arrival hyperbolic-excess velocity at Jupiter becomes

$$V_{h,2}^2 = V_J^2 + V_2^2 - 2V_J V_2(\sin \gamma_2 \sin \gamma_J + \cos \gamma_2 \cos \gamma_J \cos i_{2,J}) \tag{C7}$$

where the terms in the parentheses resulted from using the direction cosines of the vectors V_J and V_2 shown in figure 4. Jupiter's orbital velocity V_J and flight-path angle γ_J were computed from the well-known expressions:

$$V_J^2 = \frac{\mu}{r_J}\left(2 - \frac{r_J}{a_J}\right) \tag{C8}$$

$$\gamma_J = \cos^{-1}\sqrt{\frac{r_{a,J}r_{p,J}}{r_J\left(r_{a,J} + r_{p,J} - r_J\right)}} \tag{C9}$$

Upon departure from Jupiter, the inclination angle can be approximated by

$$i_{3,J} = \sin^{-1}\left(\frac{z'}{r_J \sin\theta_{3,4}}\right) \tag{C10}$$

where values from the coplanar results are utilized for r_J and $\theta_{3,4}$. The departure heliocentric velocity V_3 can be solved from the following expressions, which are similar to equation (C7):

$$V_{h,3}^2 = V_J^2 + V_3^2 - 2V_JV_3\left(\sin\gamma_3 \sin\gamma_J + \cos\gamma_3 \cos\gamma_J \cos i_{3,J}\right) \tag{C11}$$

$$\frac{r_JV_{h,3}^2}{\mu} = \frac{r_J}{\mu}\left[V_J^2 + V_3^2 - 2V_JV_3\left(\sin\gamma_3 \sin\gamma_J + \cos\gamma_3 \cos\gamma \cos i_{3,J}\right)\right] \tag{C11a}$$

If $\frac{r_JV_3^2}{\mu} < 2$ in equation (C11a), continue with equations (B19) to (B22), and if $\frac{r_JV_3^2}{\mu} > 2$, continue with equations (B23) to (B29). The departure flight-path angle γ_3 and the heliocentric radius to Saturn r_4 are used as variables in computing several trajectories from equation (C11) and the corresponding equations noted for the conditions of $\frac{r_JV_3^2}{\mu}$. These results are plotted in a manner similar to that used for the coplanar trajectories in sketch (b) of appendix B, where now γ_3 replaces $\frac{RP}{R_J}$. Then the matched values of γ_3, $\theta_{3,4}$, and $t_{3,4}$ are determined.

The remaining matched conditions can be determined for the final phase of the noncoplanar Earth-Jupiter-Saturn trajectory by employing these data in the following expressions and in equation (B15).

The angle between the arrival hyperbolic-excess velocity vector and Jupiter's plane is

$$\psi_2 = \sin^{-1}\left(\frac{V_2 \cos\gamma_2 \sin i_{2,J}}{V_{h,2}}\right) \tag{C12}$$

Likewise, the angle between the departure hyperbolic-excess velocity vector and Jupiter's plane can be expressed as

$$\psi_3 = \sin^{-1}\left(\frac{V_3 \cos \gamma_3 \sin i_{3,J}}{V_{h,3}}\right) \tag{C13}$$

The gravity-turn angle with respect to Jupiter is determined from

$$\alpha = \cos^{-1}\left(1 - \frac{Q^2}{2V_{h,3}{}^2}\right) \tag{C14}$$

REFERENCES

1. Hunter, Maxwell W. II: Future Unmanned Exploration of the Solar System. Astronaut. Aeron., vol. 2, no. 5, May 1964, pp. 16-26.

2. Niehoff, John C.: An Analysis of Gravity Assisted Trajectories to Solar System Targets. AIAA Paper No. 66-10, 1966.

3. Sohn, Robert L.: Venus Swingby Mode for Manned Mars Missions. J. Spacecraft Rockets, vol. 1, no. 5, Sept.-Oct. 1964, pp. 565-567.

4. Minovitch, Michael A.: The Determination and Characteristics of Ballistic Interplanetary Trajectories Under the Influence of Multiple Planetary Attractions. Tech. Rept. No. 32-464 (Contract No. NAS 7-100), Jet Propulsion Lab., California Inst. Technol., Oct. 31, 1963.

5. Gillespie, Rollin W.; and Ross, Stanley: The Venus Swingby Mission Mode and Its Role in the Manned Exploration of Mars. AIAA Paper no. 66-37, 1966.

6. H.M. Nautical Almanac Office: Planetary Co-Ordinates for the Years 1960-1980. Referred to the Equinox of 1950.0. Her Majesty's Stationery Office, 1958.

7. Eckert, W. J.; Brouwer, Dirk; and Clemence, G. M.: Coordinates of the Five Outer Planets 1653-2060. Astronomical Papers Prepared for the Use of the American Ephemeris and Nautical Almanac, Vol. XII, U.S. Naval Obs., 1951.

8. Flandro, G. A.: Utilization of Energy Derived From the Gravitational Field of Jupiter for Reducing Flight Time to the Outer Solar System. Supporting Research and Advanced Development, Space Programs Sum. No. 37-35, vol. IV, Jet Propulsion Lab., California Inst. Technol., Oct. 31, 1965, pp. 12-23.

9. Anon.: Erratum. Supporting Research and Advanced Development, Space Programs Sum. no. 37-36, vol. IV, Jet Propulsion Lab., California Inst. Technol., Dec. 31, 1965, p. 23.

10. Friedlander, Alan L.; and Narin, Francis: Low-Thrust Trajectory and Payload Analysis for Solar System Exploration. AIAA Paper No. 66-497, June 1966.

11. Luidens, Roger W.; and Kappraff, Jay M.: Mars Nonstop Round-Trip Trajectories. NASA TN D-2605, 1965.

12. Sturms, Francis M., Jr.; and Cutting, Elliott: Trajectory Analysis of a 1970 Mission to Mercury Via a Close Encounter With Venus. AIAA Paper No. 65-90, 1965.

13. Jensen, J.; Kraft, J. D.; and Townsend, G. E., Jr.: Orbital Mechanics. Orbital Flight Handbook, NASA SP-33, pt. 1, 1963, pp. III-i - III-87.

14. Ehricke, Krafft A.: Interplanetary Operations. Space Technology. Howard S. Seifert, ed., John Wiley & Sons, Inc., c.1959, pp. 8-65-8-71.

TABLE I.- A COMPARISON OF PRESENT COPLANAR DATA

WITH OTHER PUBLISHED RESULTS

Parameter	Present data	Results of reference 2
Launch date	Sept. 4, 1977	Sept. 1977
$V_{h,1}$, km/sec	10.52	10.52
r_J, km	7.86×10^8	7.74×10^8
$t_{1,2}$, yr	1.421	1.374
$V_{h,2}$, km/sec	12.68	12.7
R_P/R_J	4.2	4.0
r_S, km	14.14×10^8	14.15×10^8
$t_{3,4}$, yr	1.558	1.561
$V_{h,4}$, km/sec	17.77	17.8

TABLE II.- COMPARISON OF COPLANAR WITH NONCOPLANAR TRAJECTORIES

Parameter	Sept. 5, 1977 launch		Nov. 8, 1979 launch	
	Coplanar	Noncoplanar	Coplanar	Noncoplanar
[a]$V_{h,1}$, km/sec	10.363	10.363	10.363	10.363
[a]γ_1, deg	0	0	0	0
[a]$t_{1,2}$, yr	1.456	1.456	1.526	1.526
[a]$\theta_{1,2}$, deg	143.53	143.53	144.70	144.70
$\Delta V_{h,1}$, km/sec	0	0.0014	0	0.0893
$i_{1,E}$, deg	0	0.94	0	2.26
V_J, km/sec	12.954	12.850	12.757	12.449
γ_J, deg	0	2.61	0	0.51
[a]V_2, km/sec	13.144	13.144	12.770	12.770
[a]γ_2, deg	54.72	54.72	54.78	54.78
$i_{2,J}$, deg	0	1.93	0	1.85
ψ_2, deg	0	1.28	0	1.18
$V_{h,2}$, km/sec	11.996	11.429	11.744	11.510
V_3, km/sec	24.462	24.004	14.859	14.584
γ_3, deg	10.91	10.65	49.62	50.08
$i_{3,J}$, deg	0	1.23	0	2.90
ψ_3, deg	0	2.54	0	2.36
$t_{3,4}$, yr	1.596	1.628	2.337	2.285
$\theta_{3,4}$, deg	53.65	54.05	26.42	25.80
α, deg	93.85	98.00	11.87	11.08
R_P/R_J	4.65	4.51	114.0	128.0

[a]Quantities assumed to have the same values for both coplanar and noncoplanar trajectories.

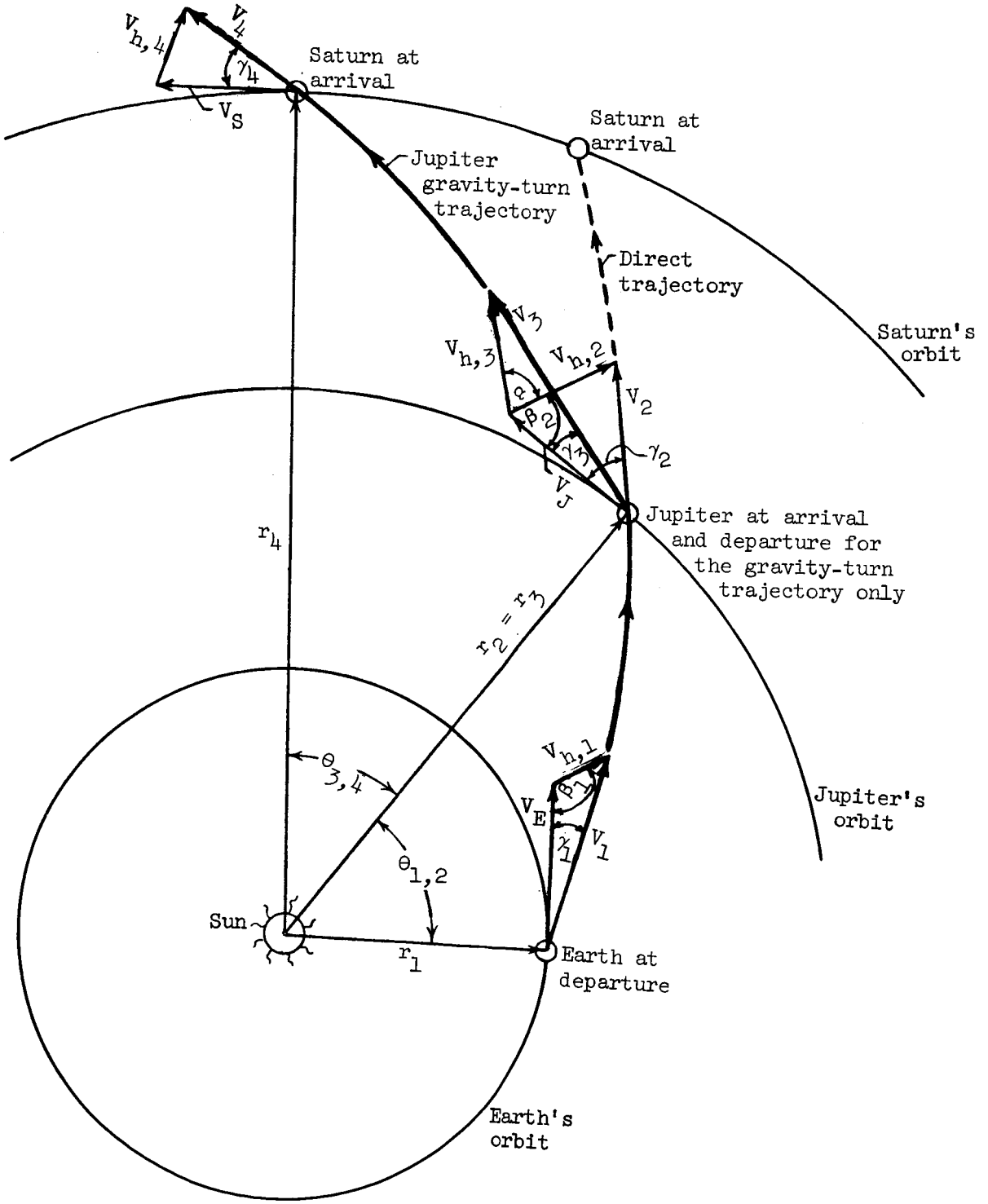

Figure 1.- Coplanar geometric relations of heliocentric trajectories and planetary configurations.

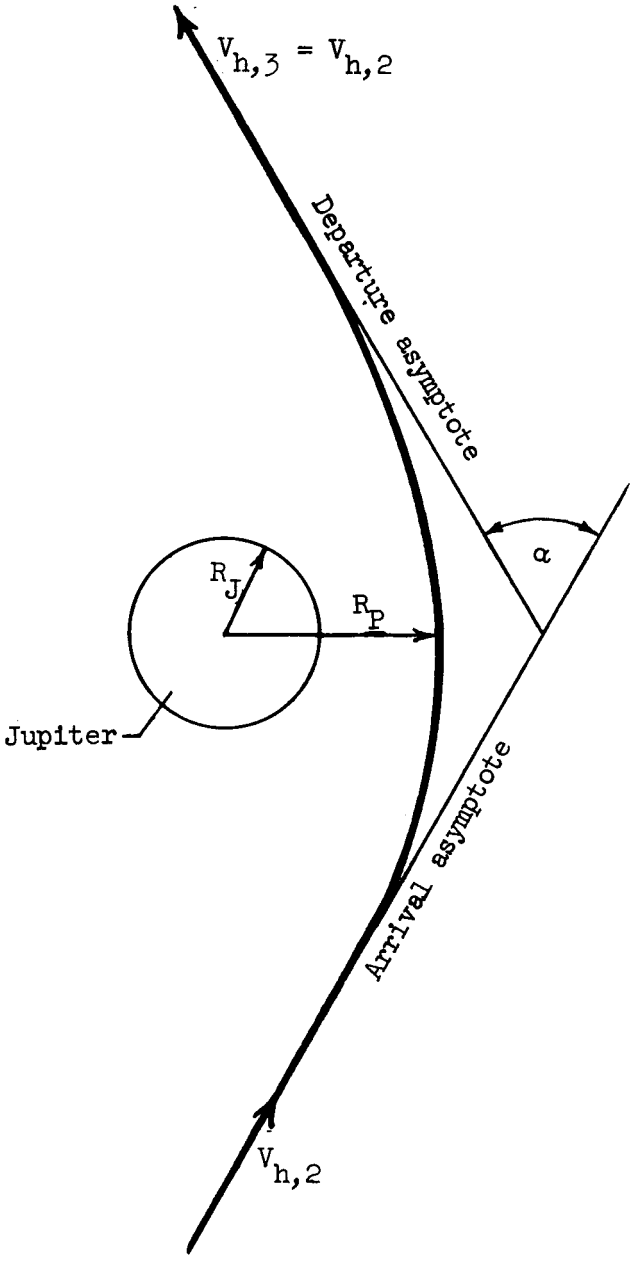

Figure 2.- Geometry of coplanar gravity-turn trajectory with respect to Jupiter.

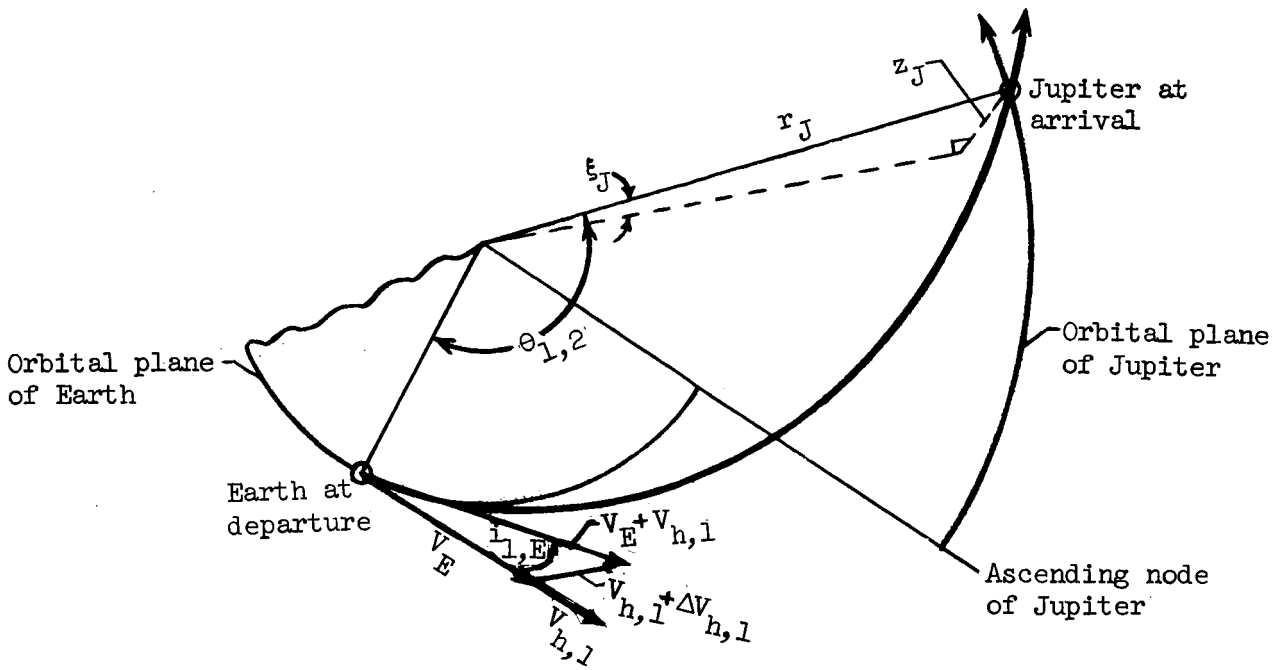

(a) Plane change at Earth.

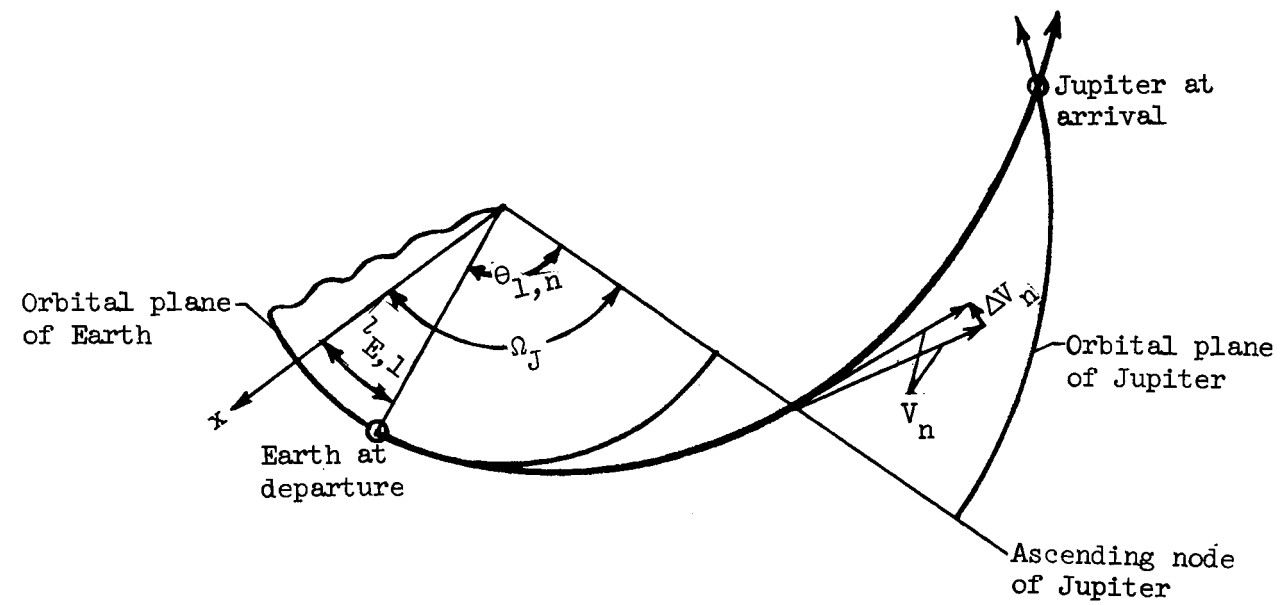

(b) Plane change at Jupiter's node.

Figure 3.- Geometry used to describe velocity increment required to change orbital plane. $\gamma_1 = 0^0$.

——— In orbital plane of Jupiter
——— - In orbital plane of spacecraft
----- Between orbital planes

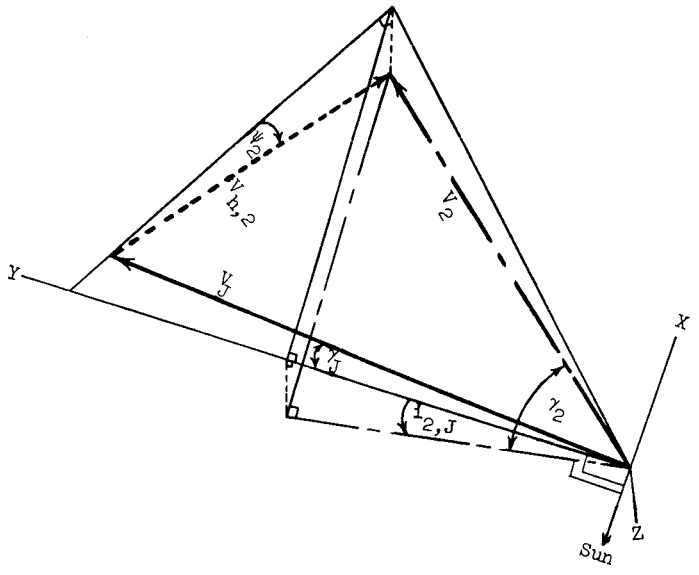

(a) Arrival at Jupiter.

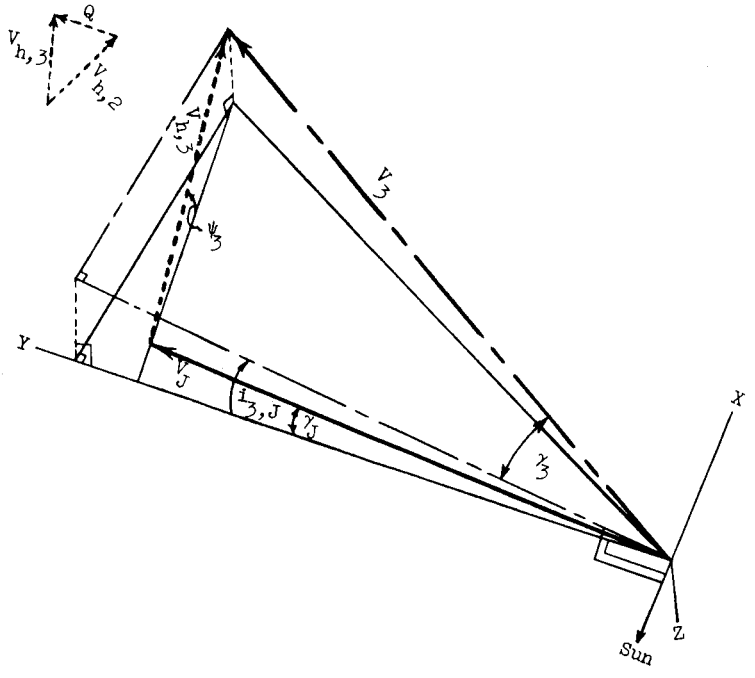

(b) Departure from Jupiter.

Figure 4.- Geometry used to describe noncoplanar trajectories at Jupiter.

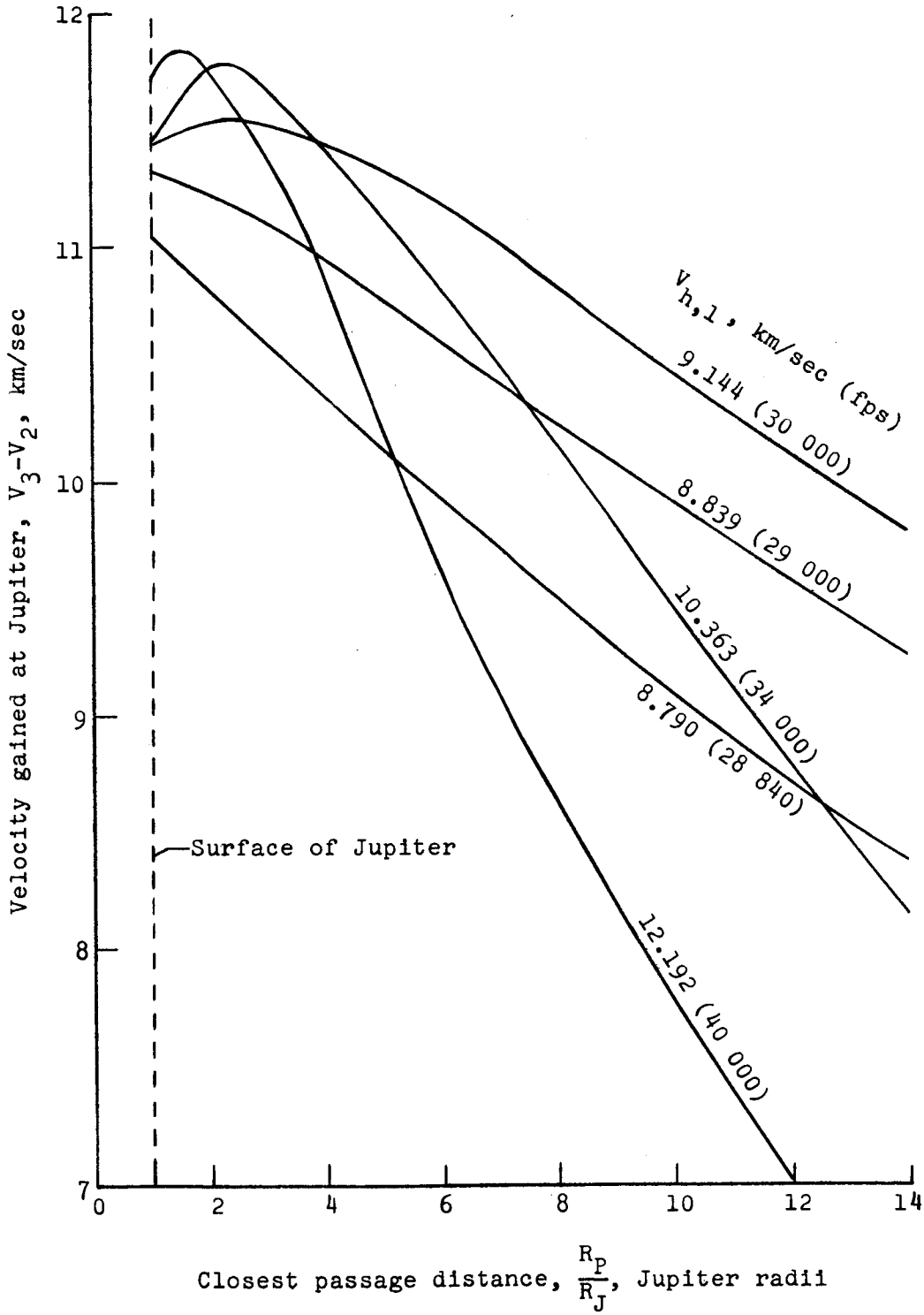

Figure 5.- Effect of passage distance on velocity gained by spacecraft at Jupiter. $\gamma_1 = 0^0$; circular orbits for planets.

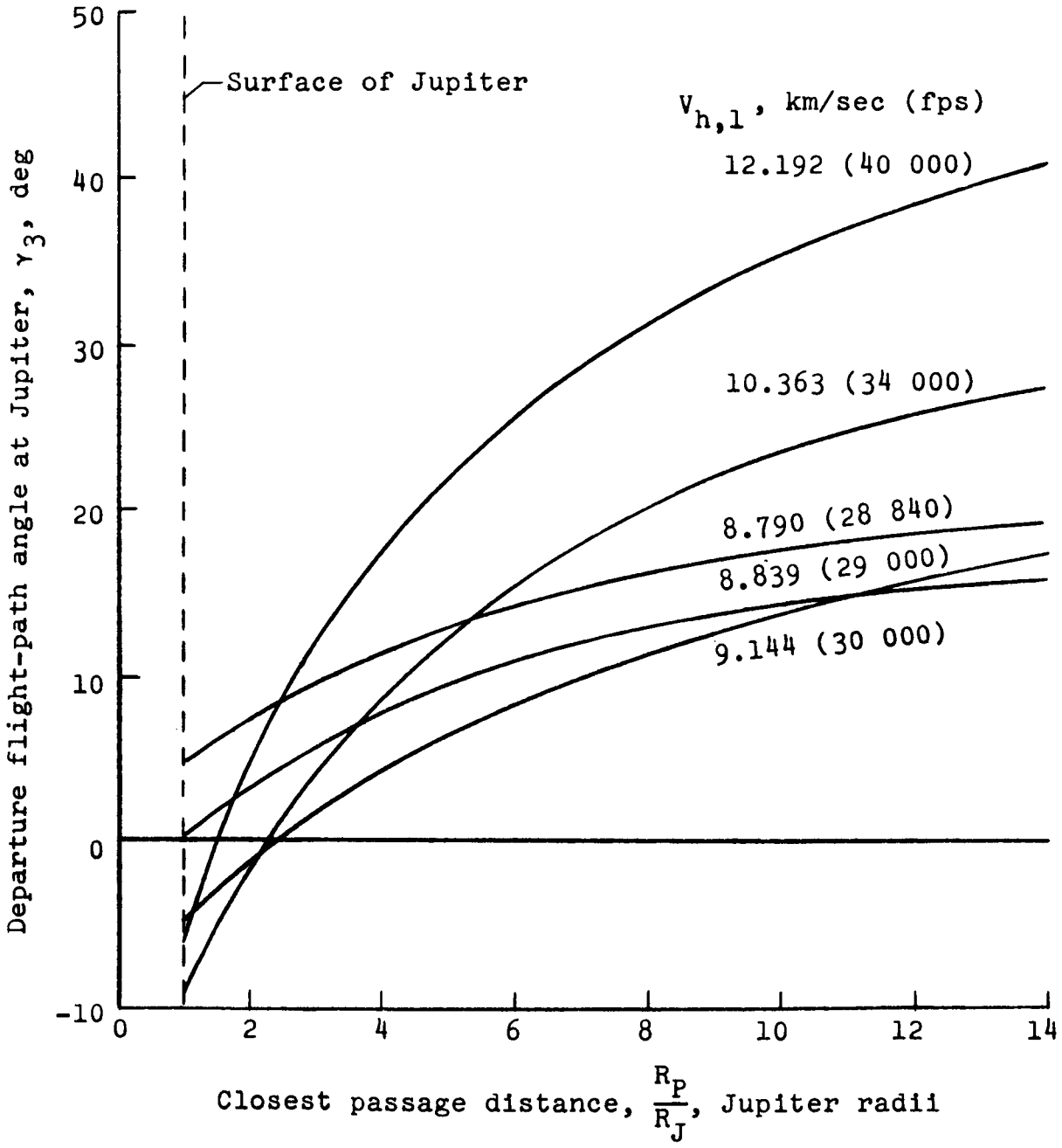

Figure 6.- Effect of passage distance on flight-path angle at Jupiter. $\gamma_1 = 0^o$; circular orbits for planets.

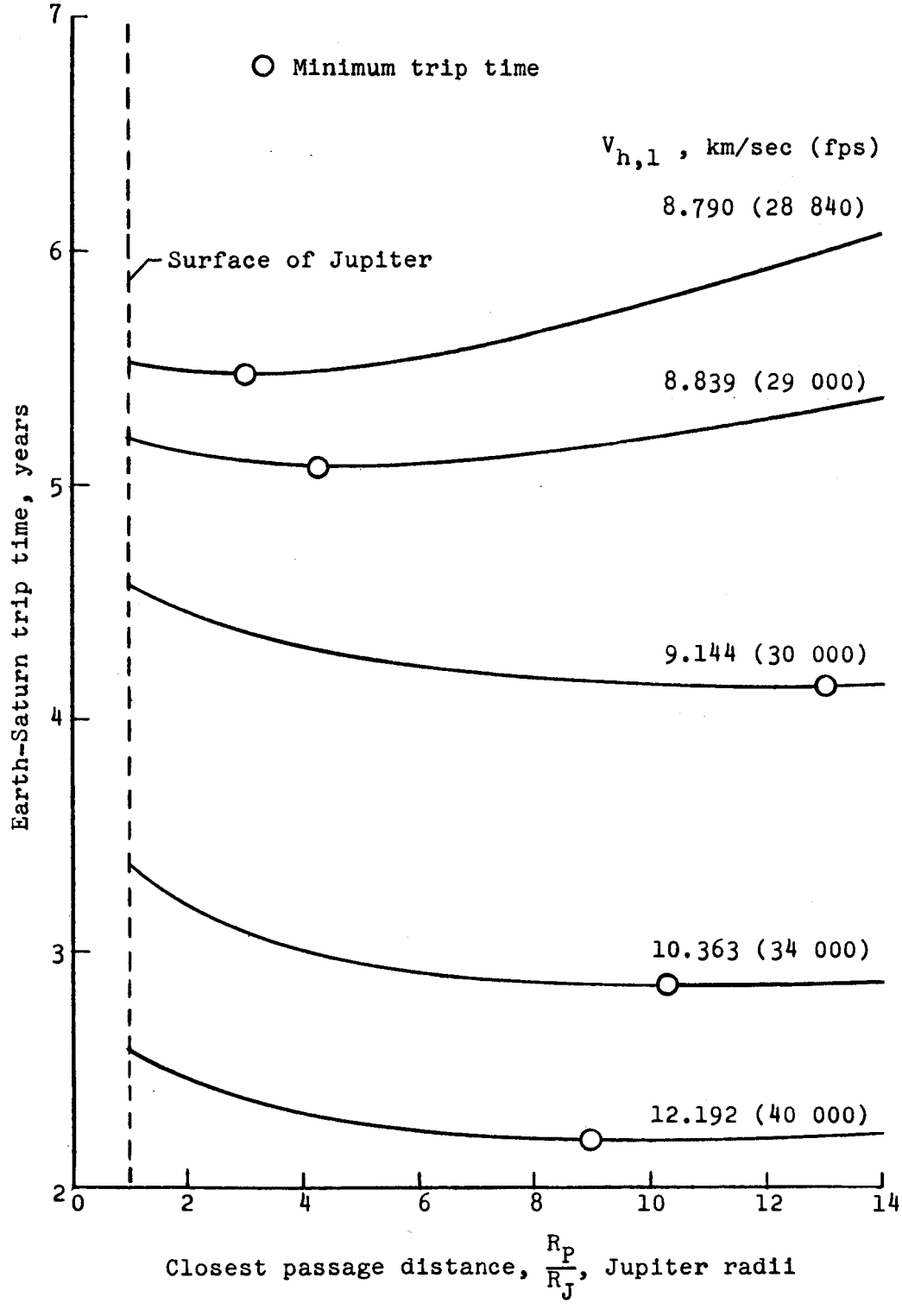

Figure 7.- Effect of passage distance at Jupiter on trip time to Saturn. $\gamma_1 = 0^0$; circular orbits for planets.

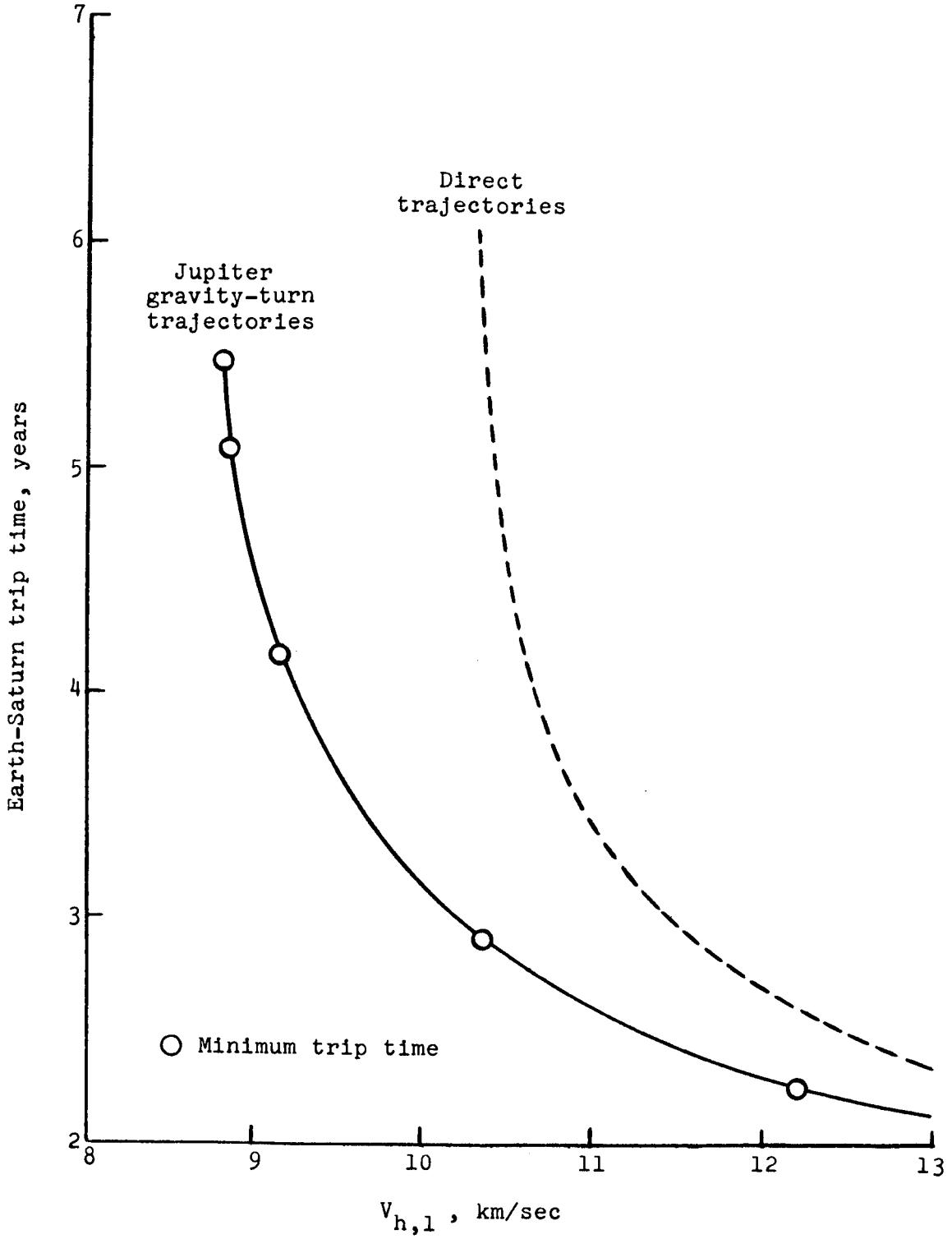

Figure 8.- Comparison of Jupiter gravity-turn with direct trajectories to Saturn in terms of trip time and velocity requirements. $\gamma_1 = 0^0$; circular orbits for planets.

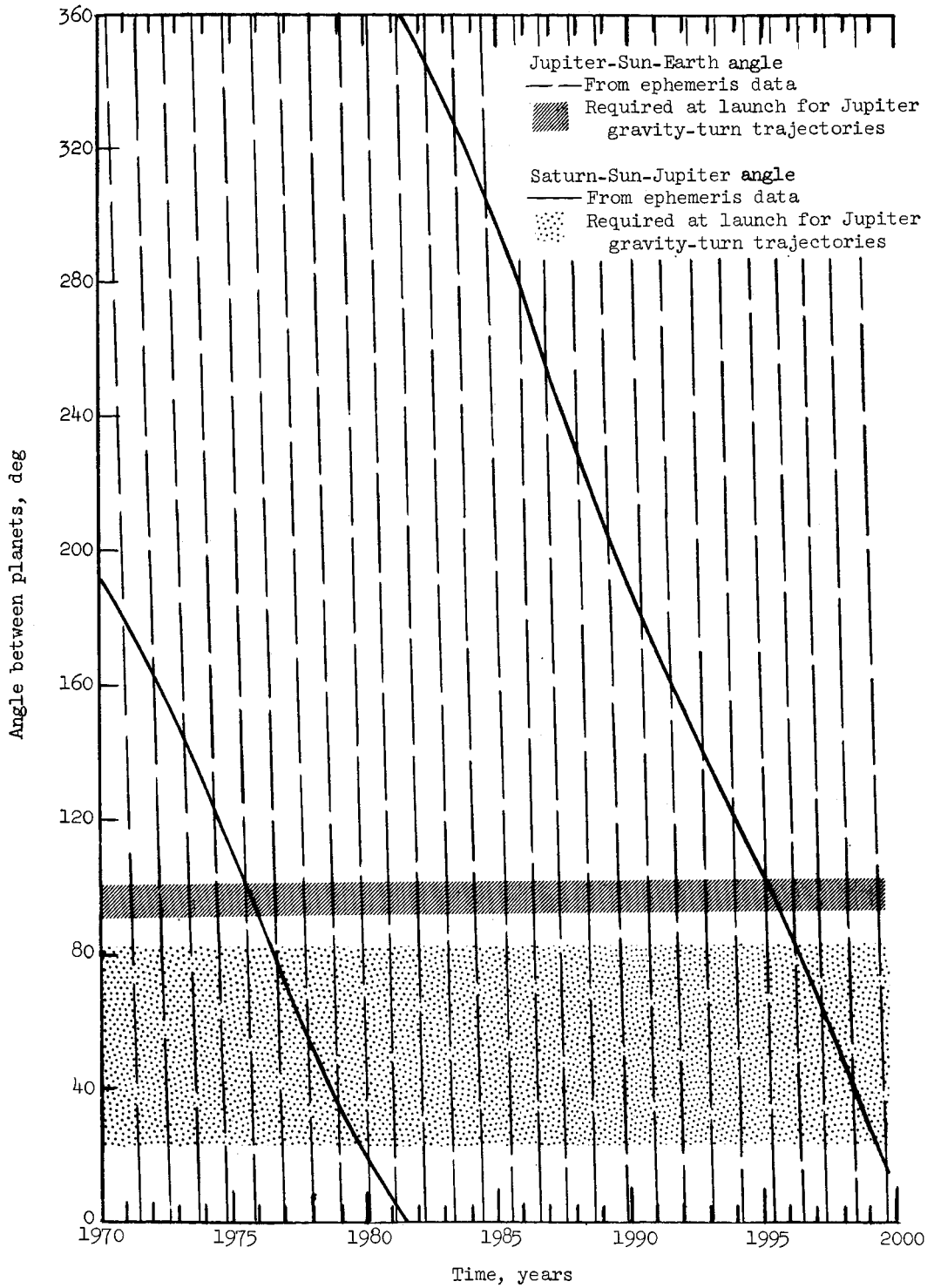

Figure 9.- Relative positions of planets with time and approximate angle requirements of planets at launch time for Jupiter gravity-turn trajectories to Saturn. $V_{h,1}$ = 10.363 km/sec (34 000 fps) to 12.192 km/sec (40 000 fps); $\gamma_1 = 0^0$.

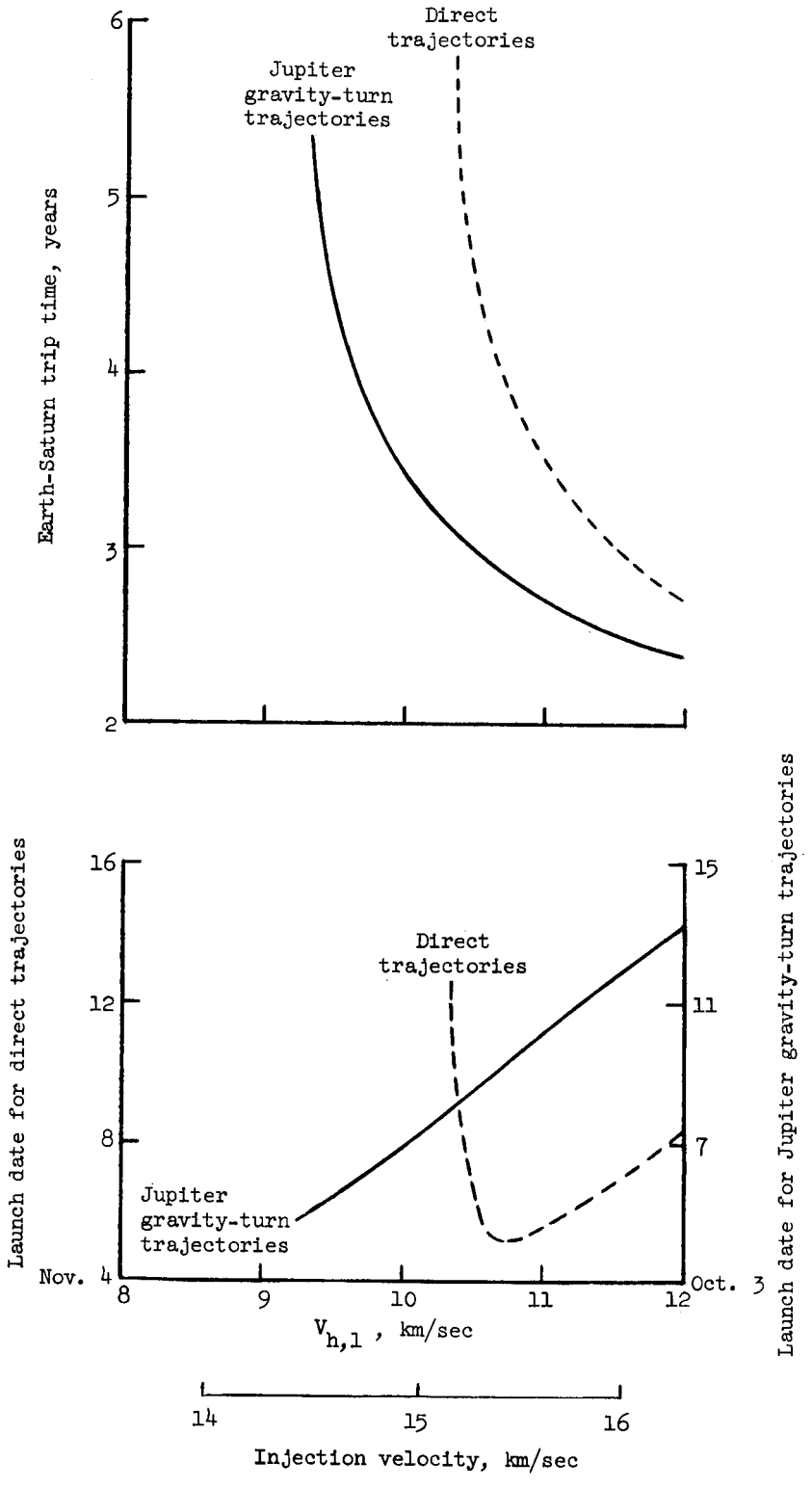

Figure 10.- Effect of hyperbolic-excess velocity at Earth on trip time and launch opportunity in 1978. $\gamma_1 = 0^0$.

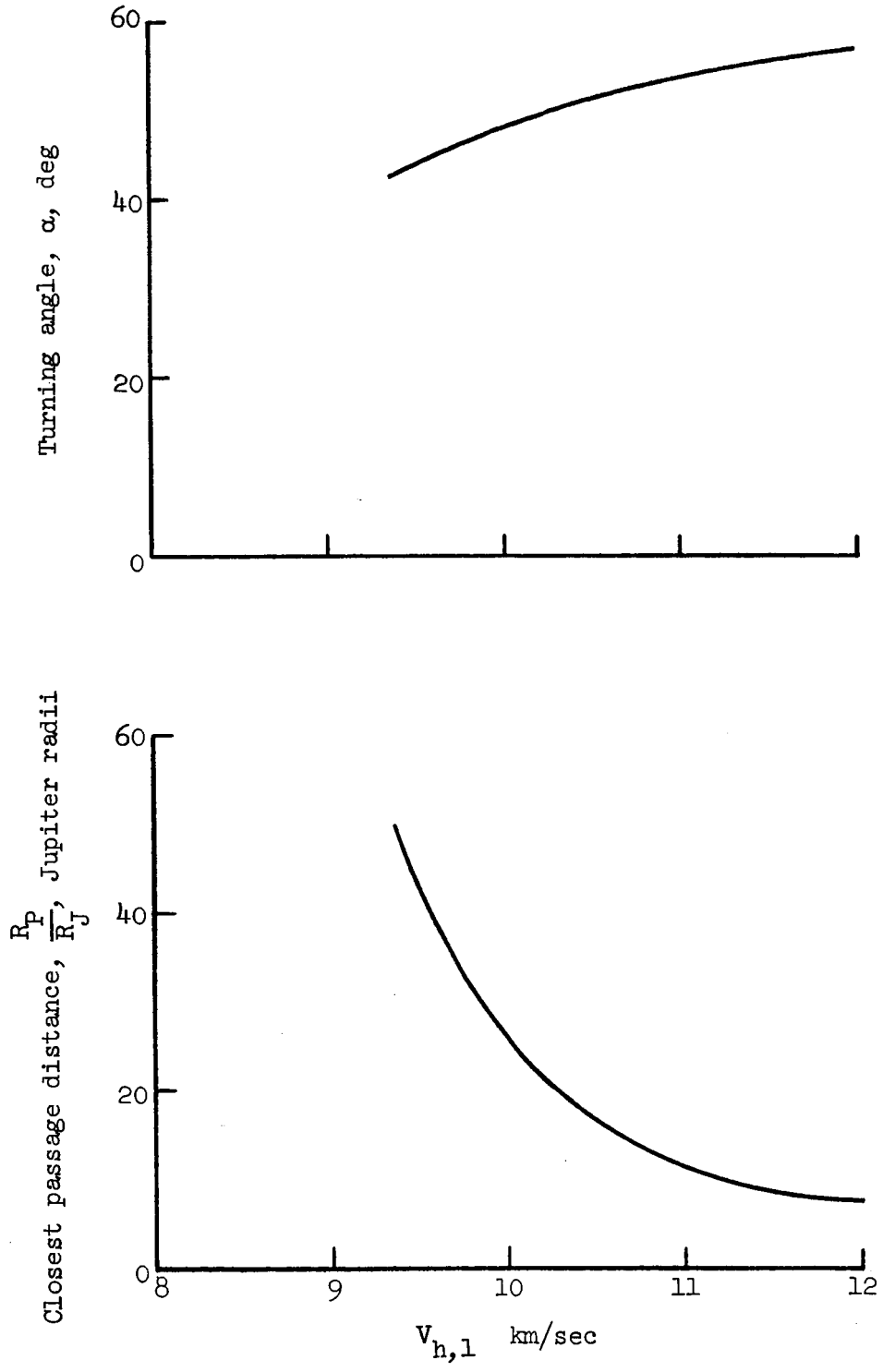

Figure 11.- Effect of hyperbolic-excess velocity for 1978 launches on turning angle and on passage distance at Jupiter. $\gamma_1 = 0^o$.

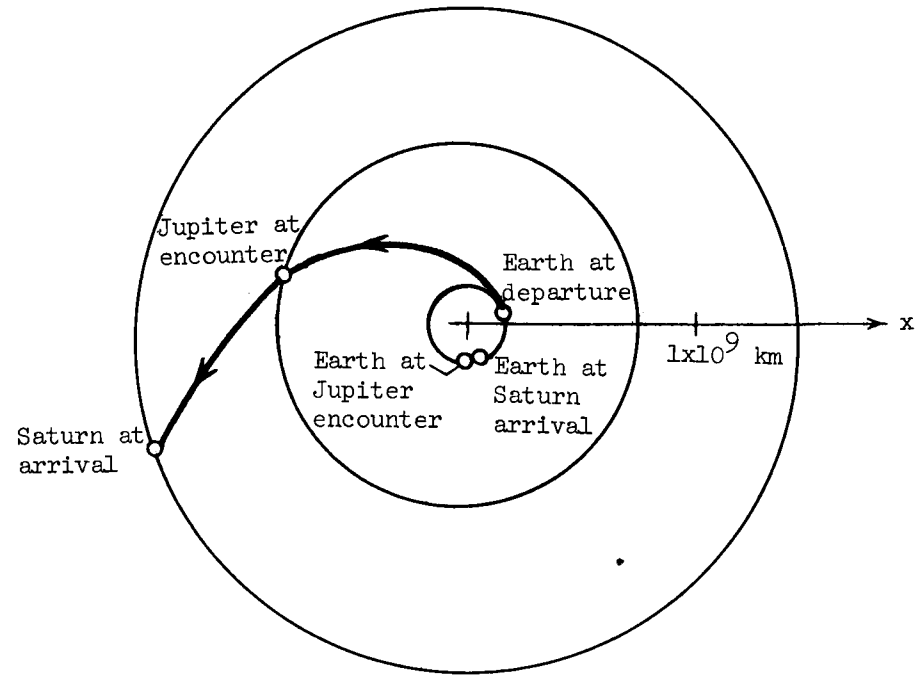

(a) $V_{h,1}$ = 9.754 km/sec (32 000 fps).

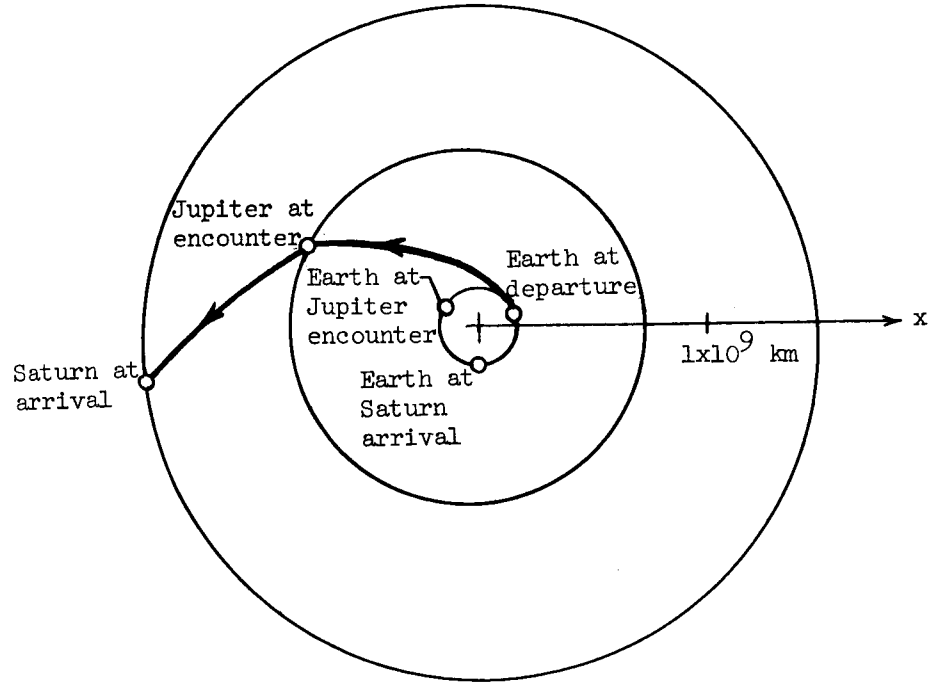

(b) $V_{h,1}$ = 10.973 km/sec (36 000 fps).

Figure 12.- Effect of hyperbolic-excess velocity on profiles of gravity-turn trajectories and their relationship to the planets. Launch year, 1978.

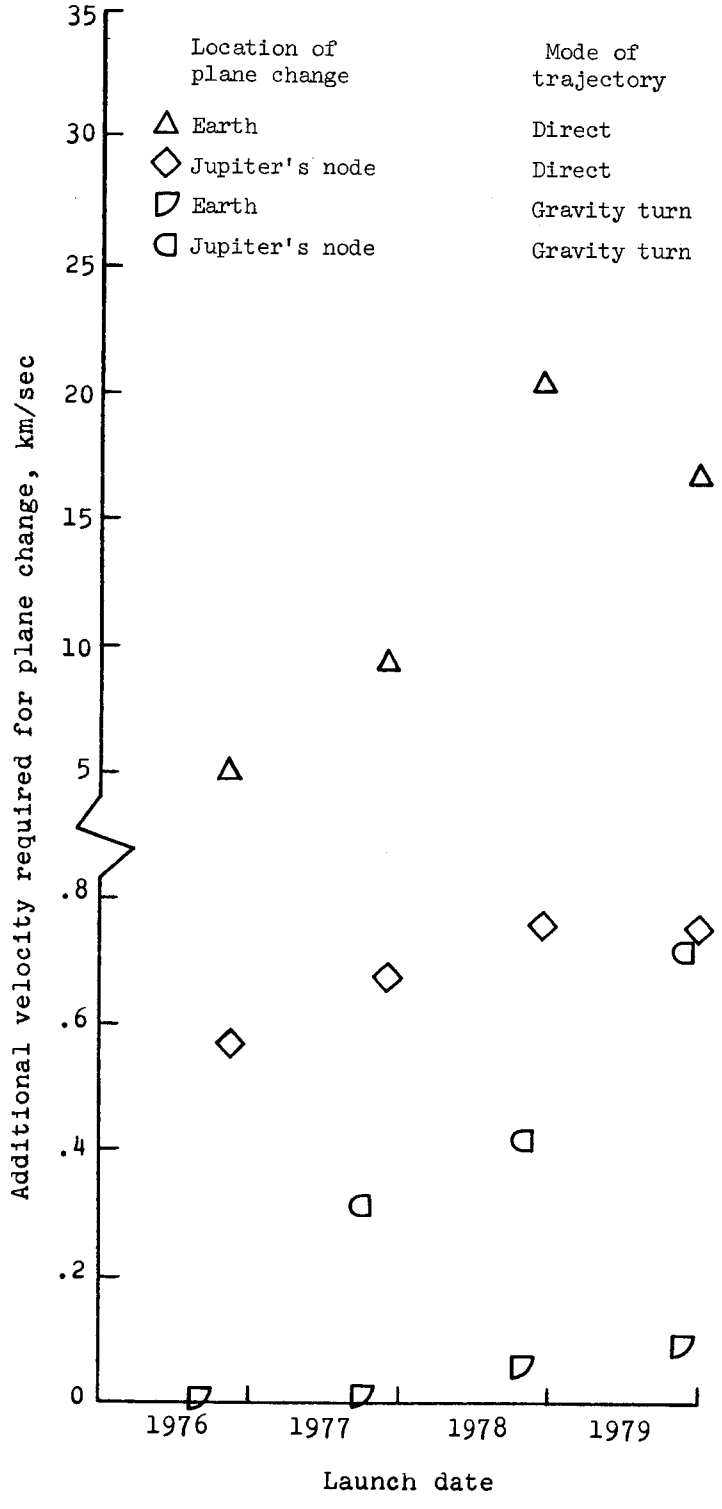

Figure 13.- Effect of plane-change location and trajectory mode on additional velocity requirement for noncoplanar transfers to Saturn. $V_{h,1}$ = 10.363 km/sec (34 000 fps); $\gamma_1 = 0^0$.

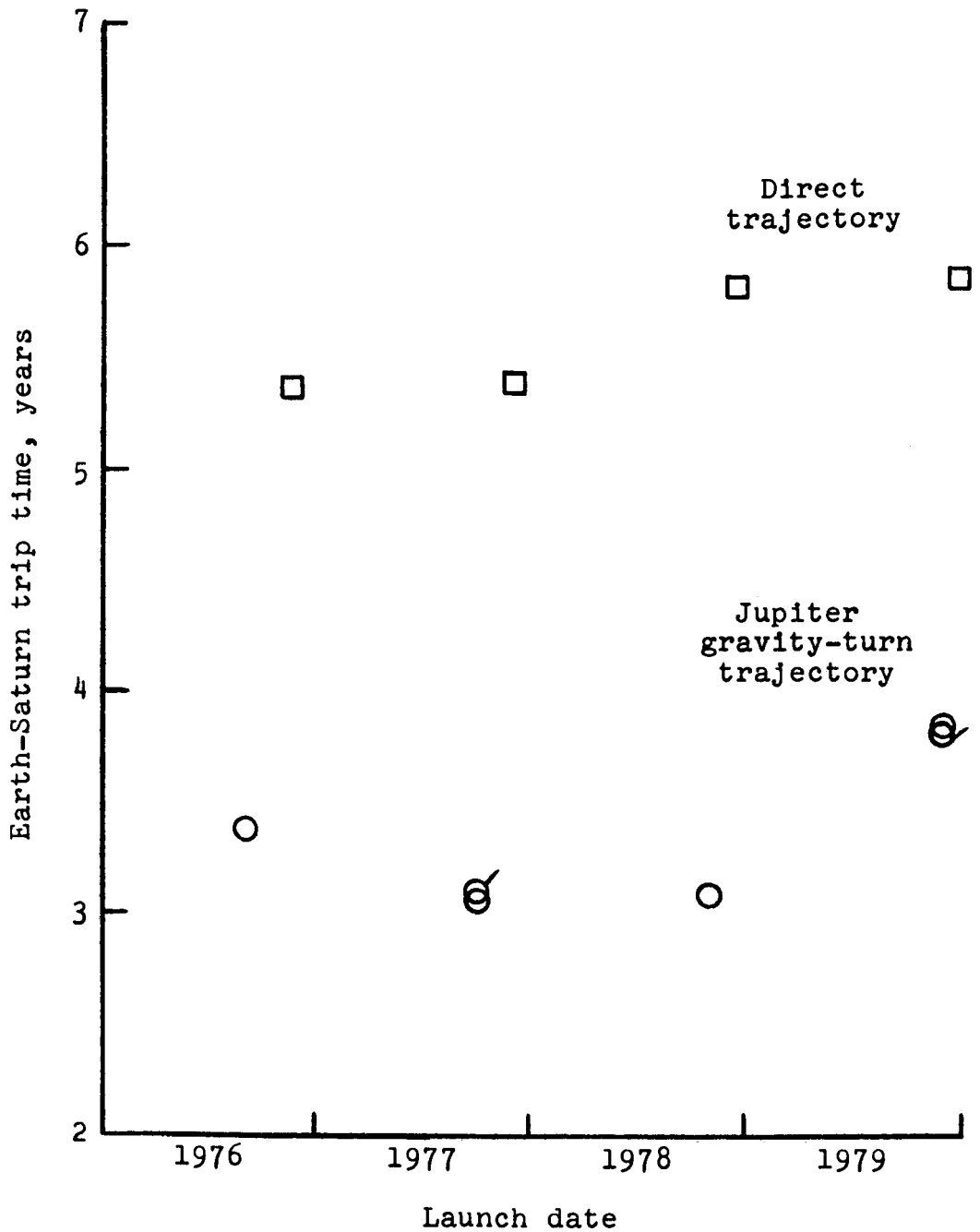

Figure 14.- Effect of Jupiter gravity-turn trajectory on trip time to Saturn for launches during four consecutive years. $V_{h,1}$ = 10.363 km/sec (34 000 fps). Flagged symbols represent noncoplanar results.

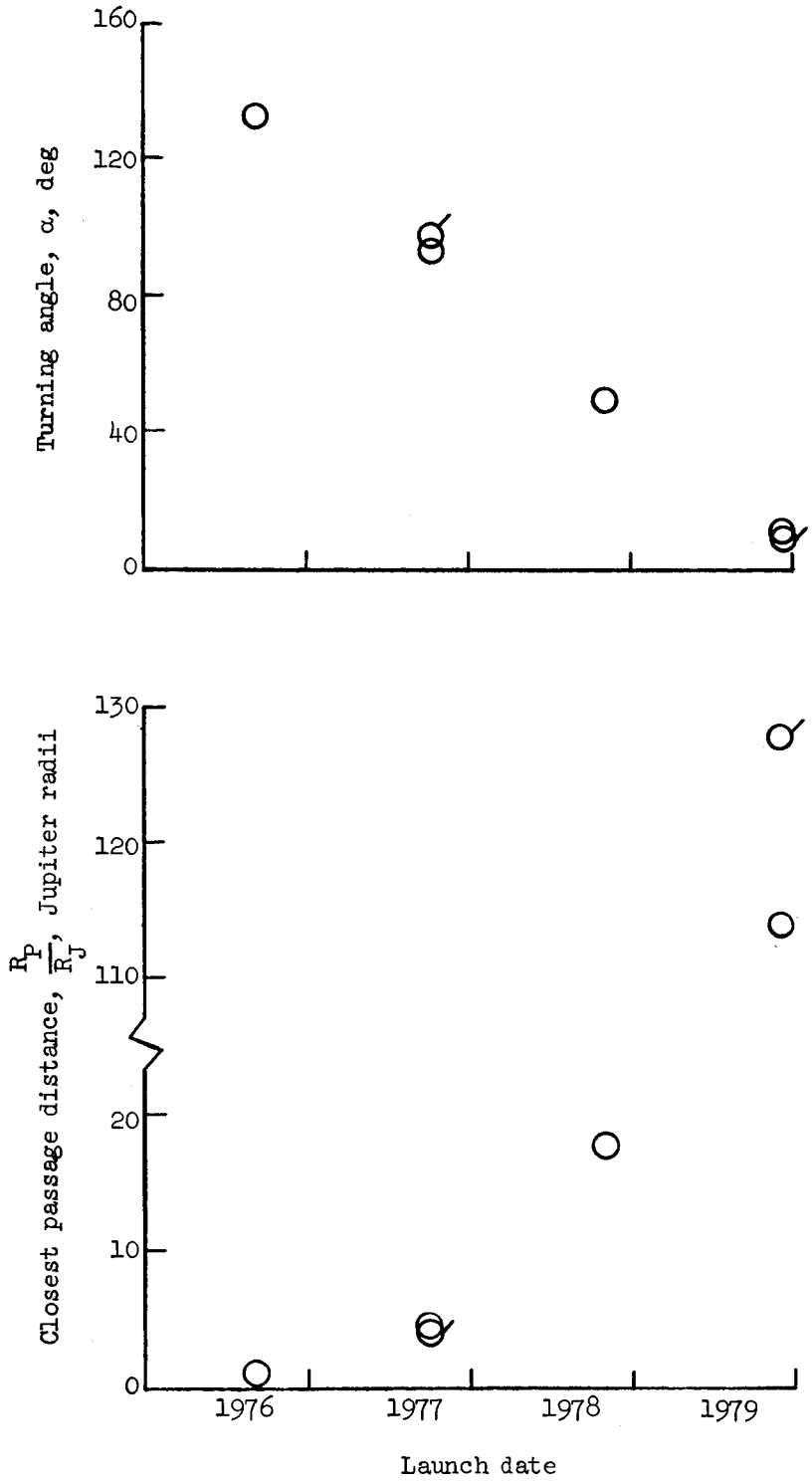

Figure 15.- Effect of launch date on turning angle and on passage distance at Jupiter. $V_{h,1}$ = 10.363 km/sec (34 000 fps); $\gamma_1 = 0^0$. Flagged symbols represent noncoplanar results.

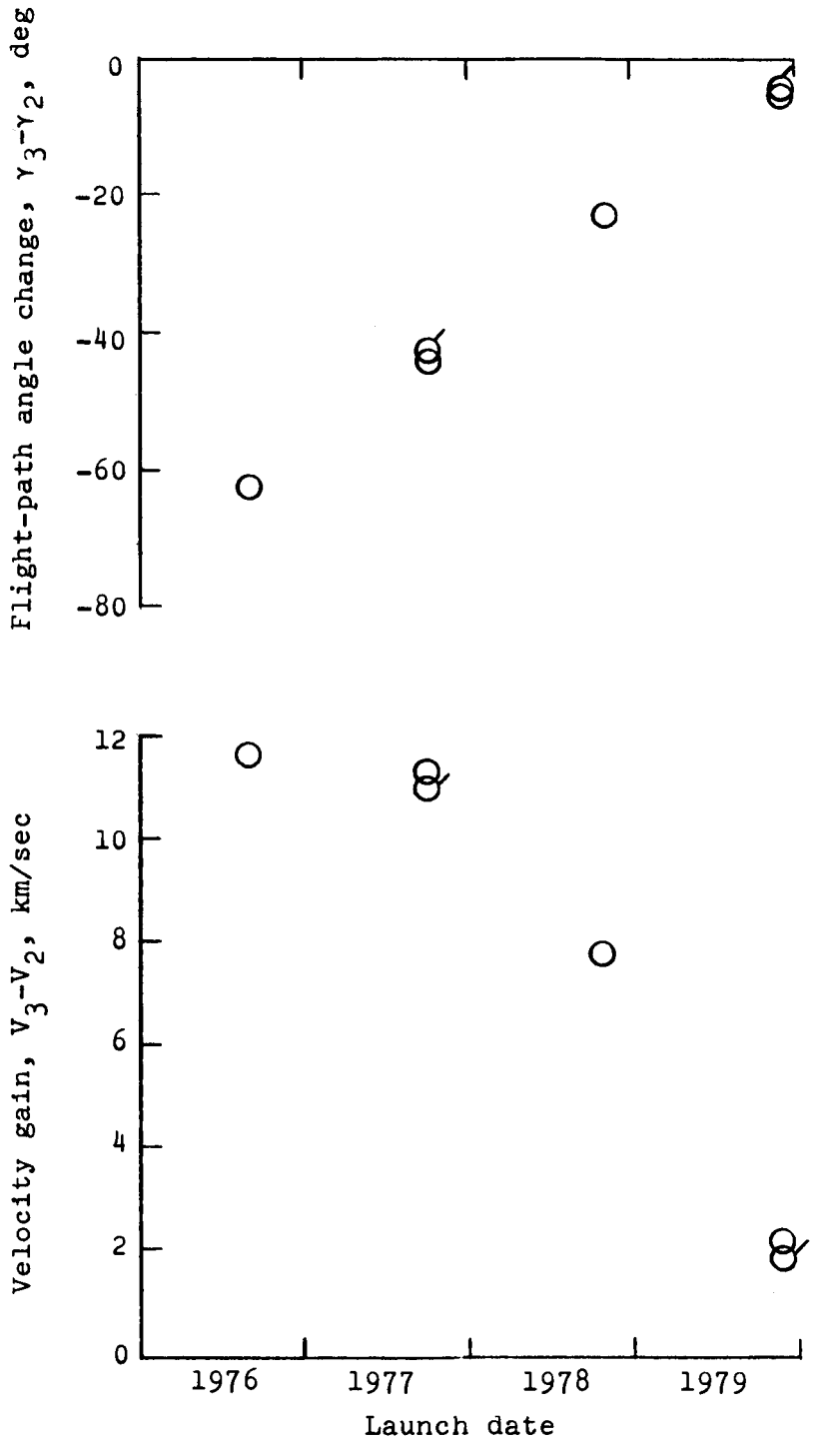

Figure 16.- Effect of launch date on change in both direction and magnitude of heliocentric velocity vector as spacecraft encounters Jupiter. $V_{h,1}$ = 10.363 km/sec (34 000 fps); $\gamma_1 = 0^0$. Flagged symbols represent noncoplanar results.

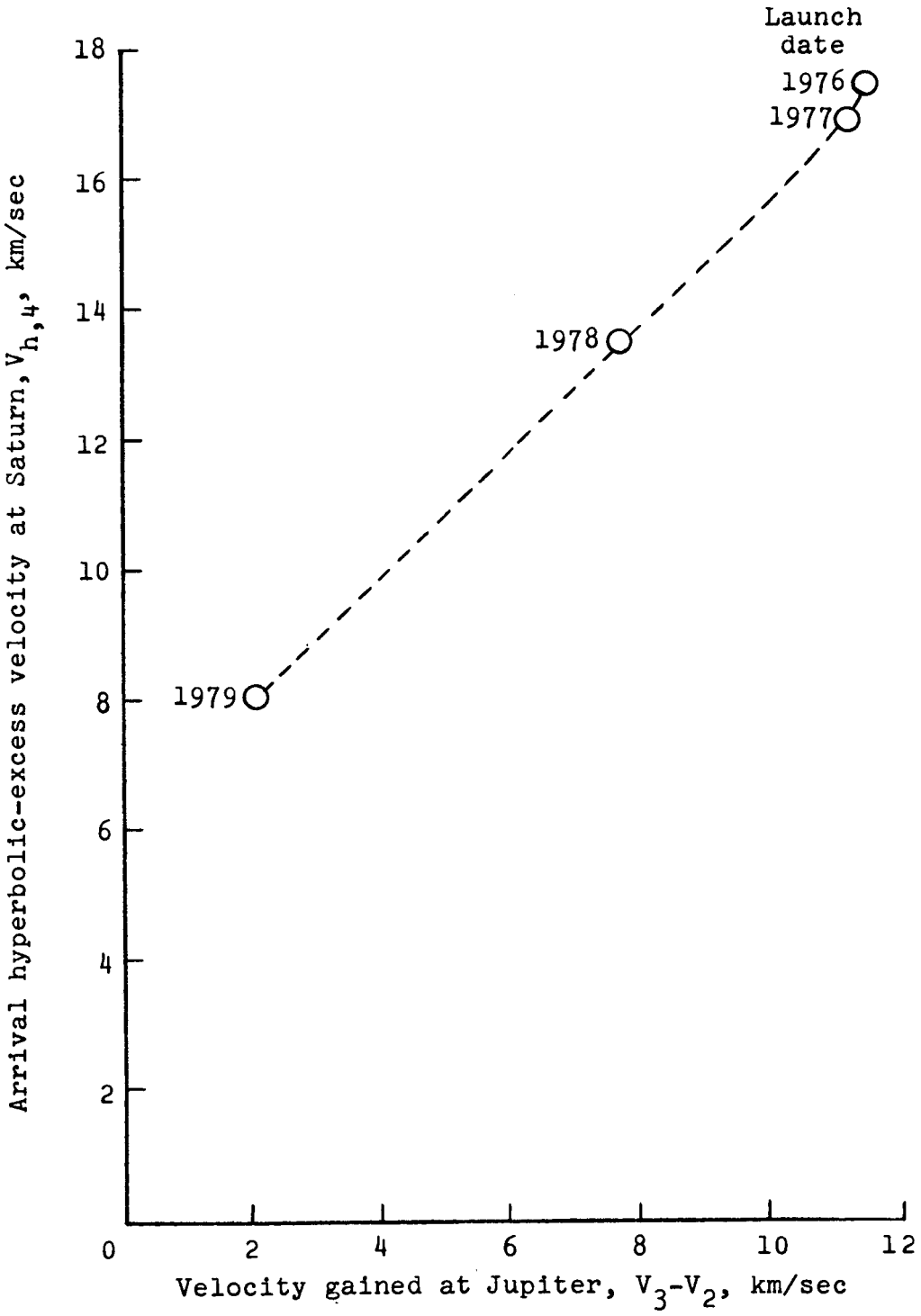

Figure 17.- Effect of increase in velocity of spacecraft at Jupiter on arrival hyperbolic-excess velocity at Saturn. $V_{h,1}$ = 10.363 km/sec (34 000 fps); $\gamma_1 = 0^0$.

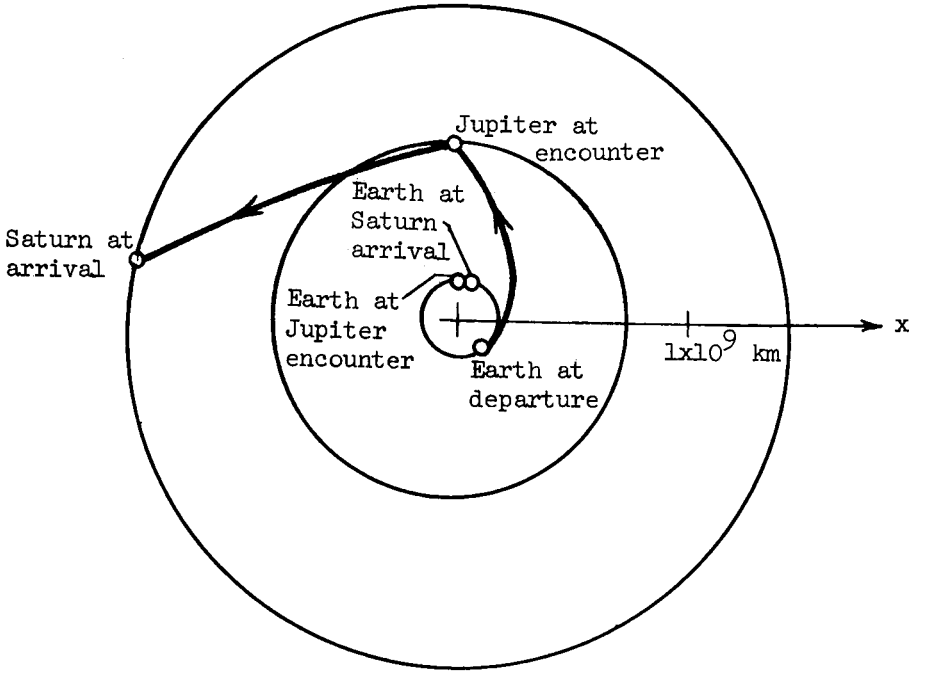

(a) 1976 launch.

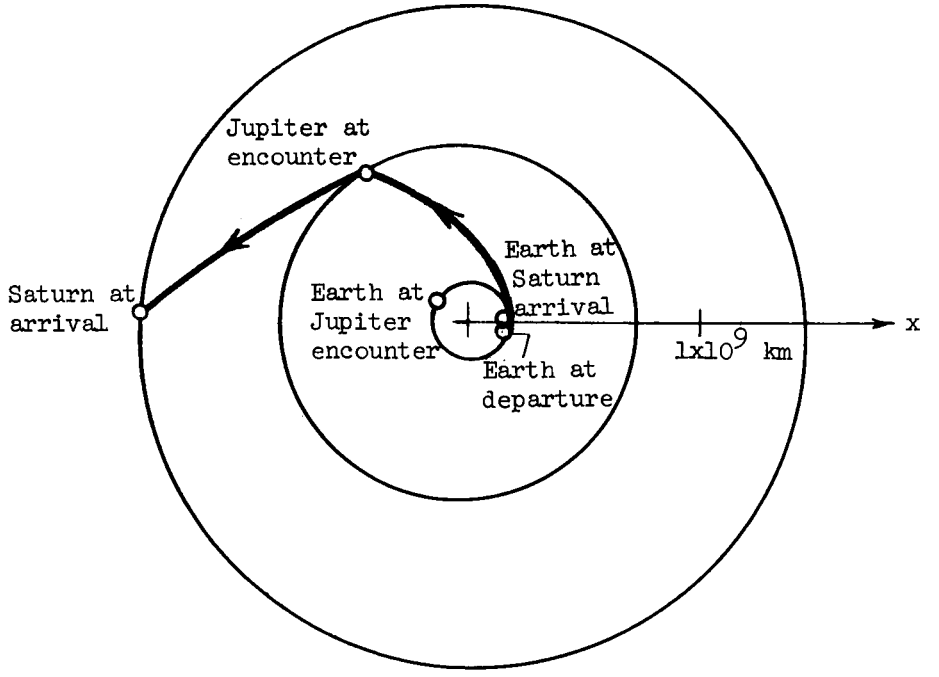

(b) 1977 launch.

Figure 18.- Profiles of Earth-Jupiter-Saturn trajectories for 1976 to 1979 launches. $V_{h,1}$ = 10.363 km/sec (34 000 fps); $\gamma_1 = 0^\circ$.

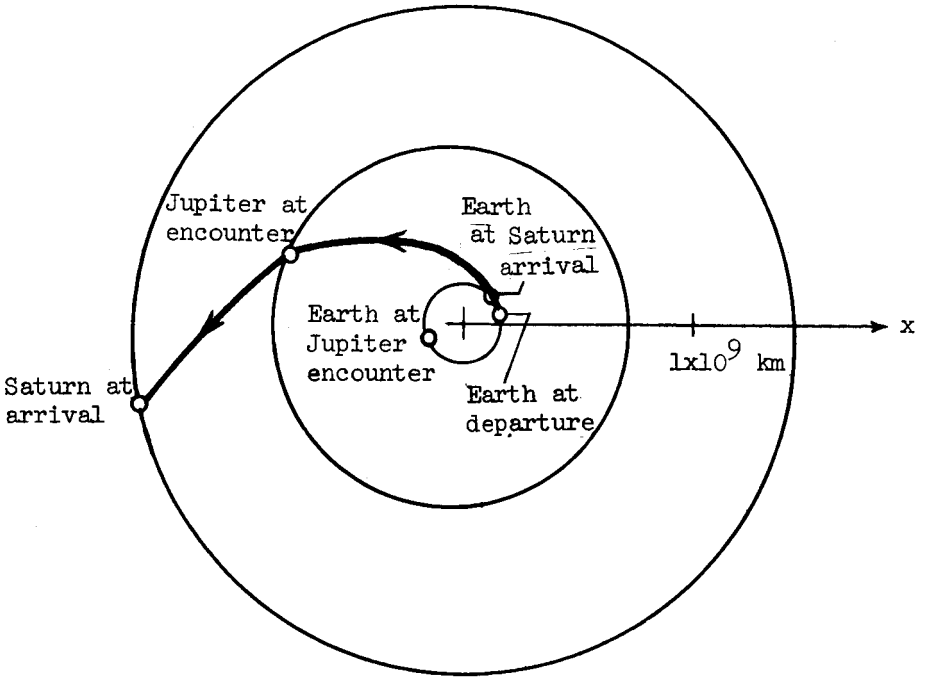

(c) 1978 launch.

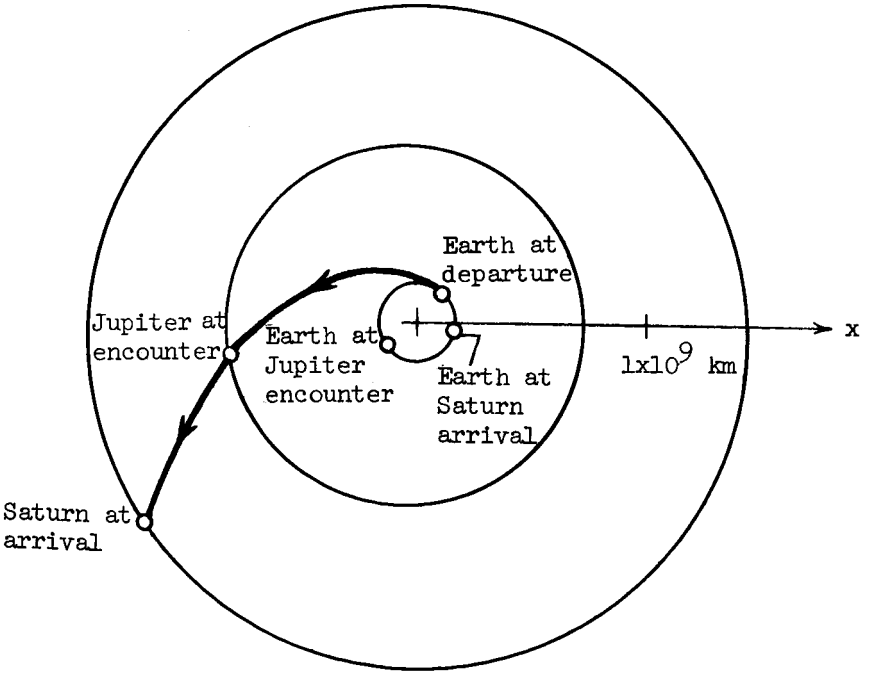

(d) 1979 launch.

Figure 18.- Concluded.

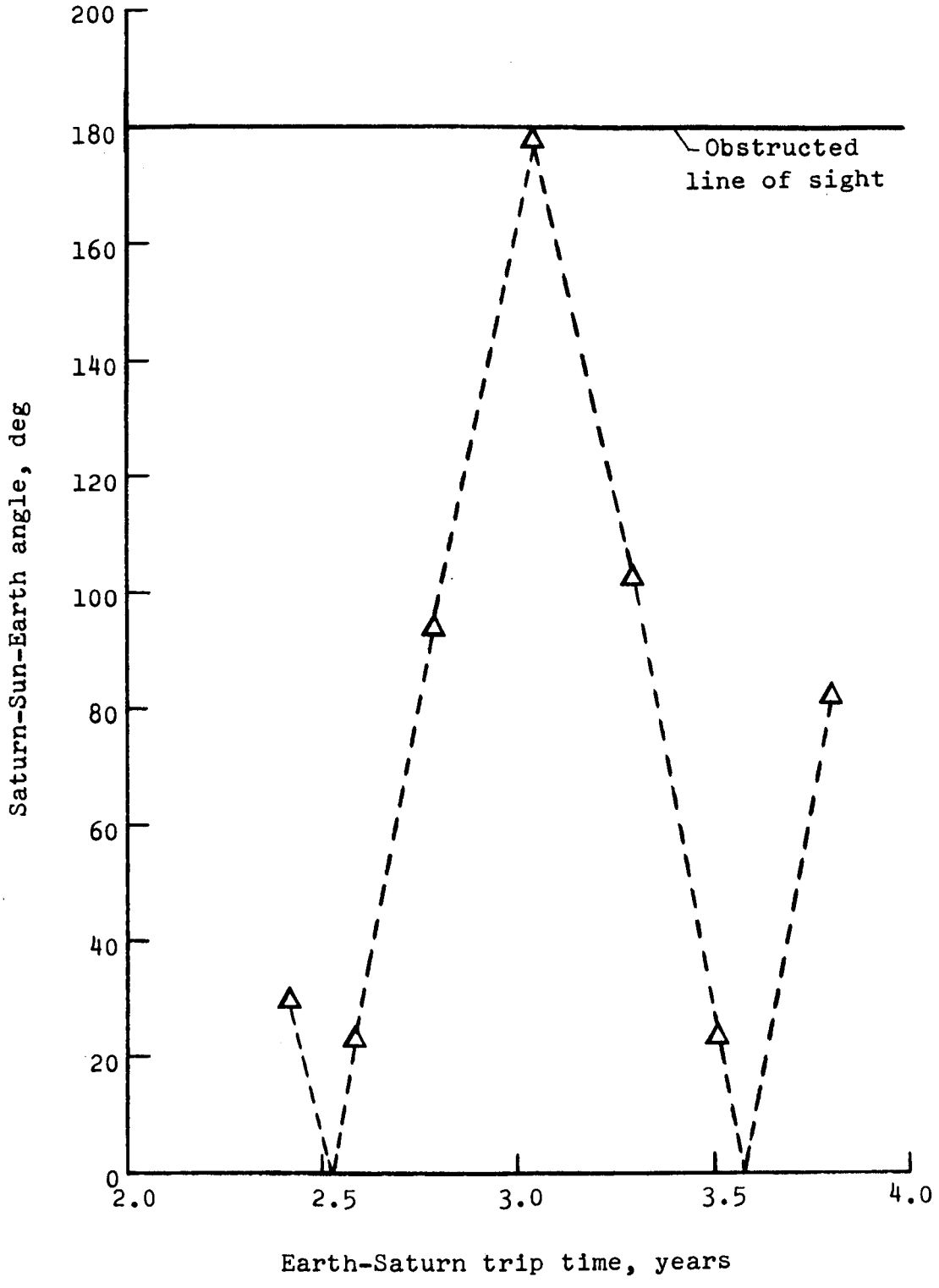

Figure 19.- Effect of trip time on Saturn-Sun-Earth angles at time of arrival at Saturn. $\gamma_1 = 0^0$; launch year, 1977.

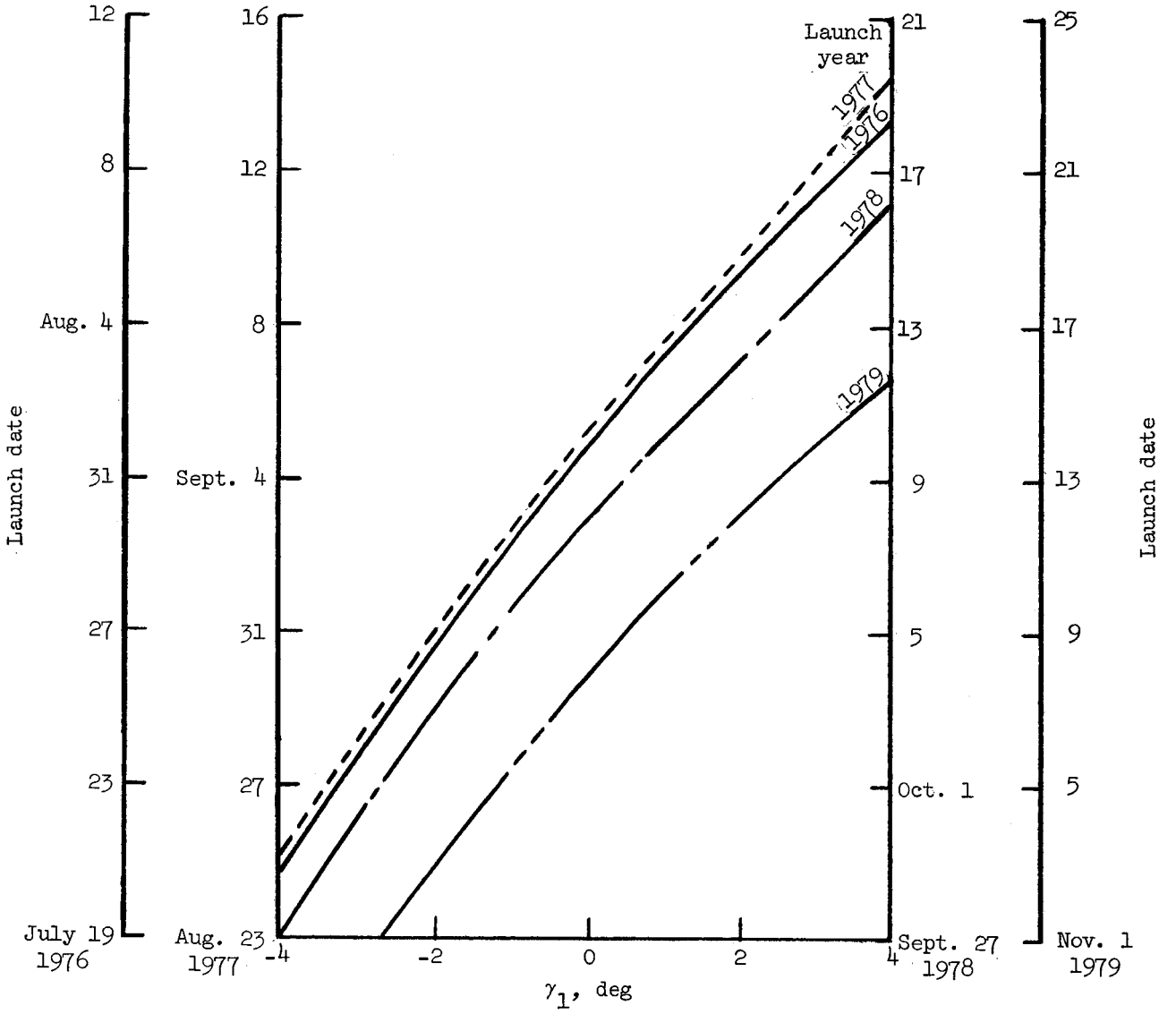

Figure 20. Effect of flight-path angle at Earth departure on launch window. $V_{h,1}$ = 10.363 km/sec (34 000 fps).

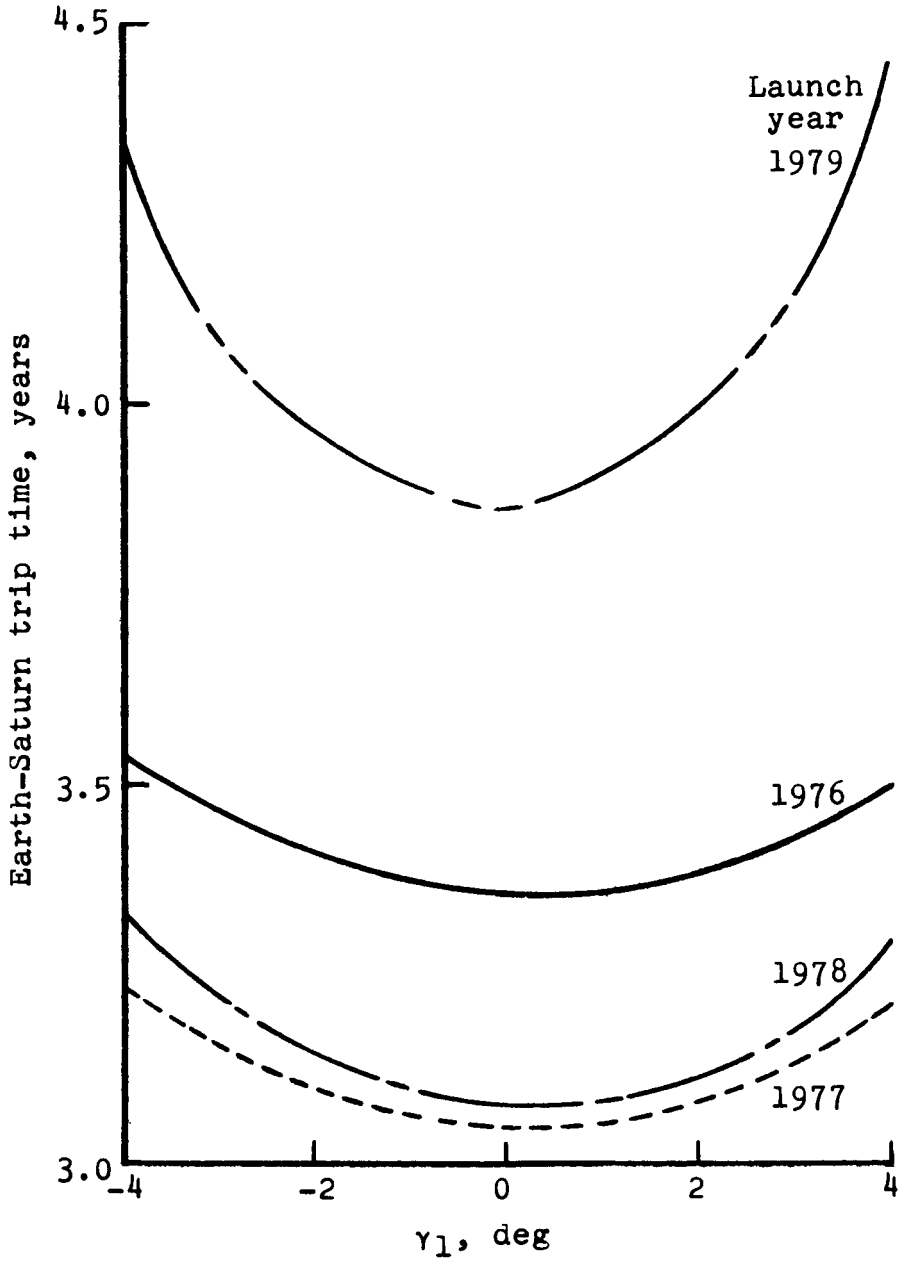

Figure 21.- Effect of flight-path angle at Earth departure on trip time. $V_{h,1}$ = 10.363 km/sec (34 000 fps).

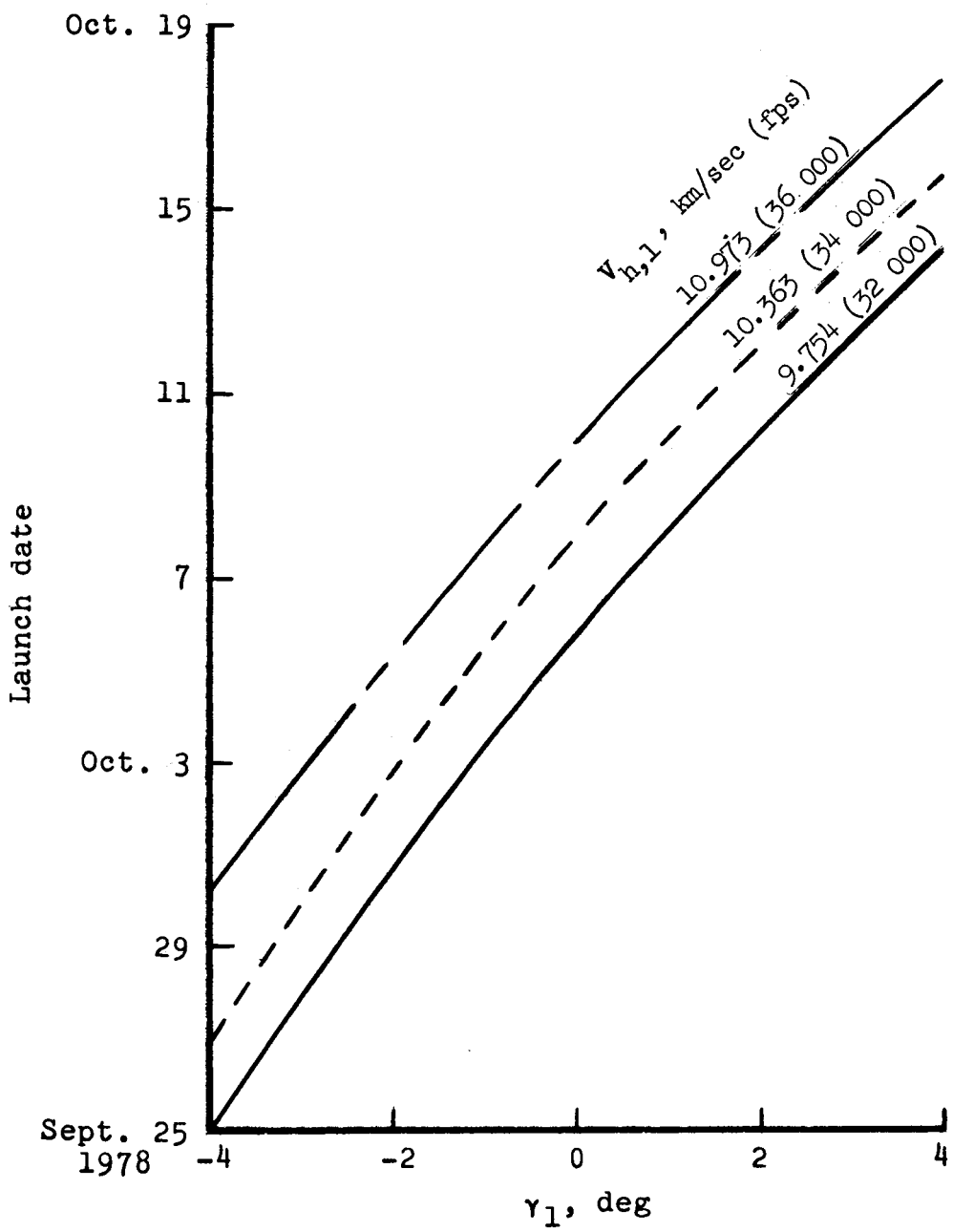

Figure 22.- Effect of hyperbolic-excess velocity and flight-path angle on launch window.

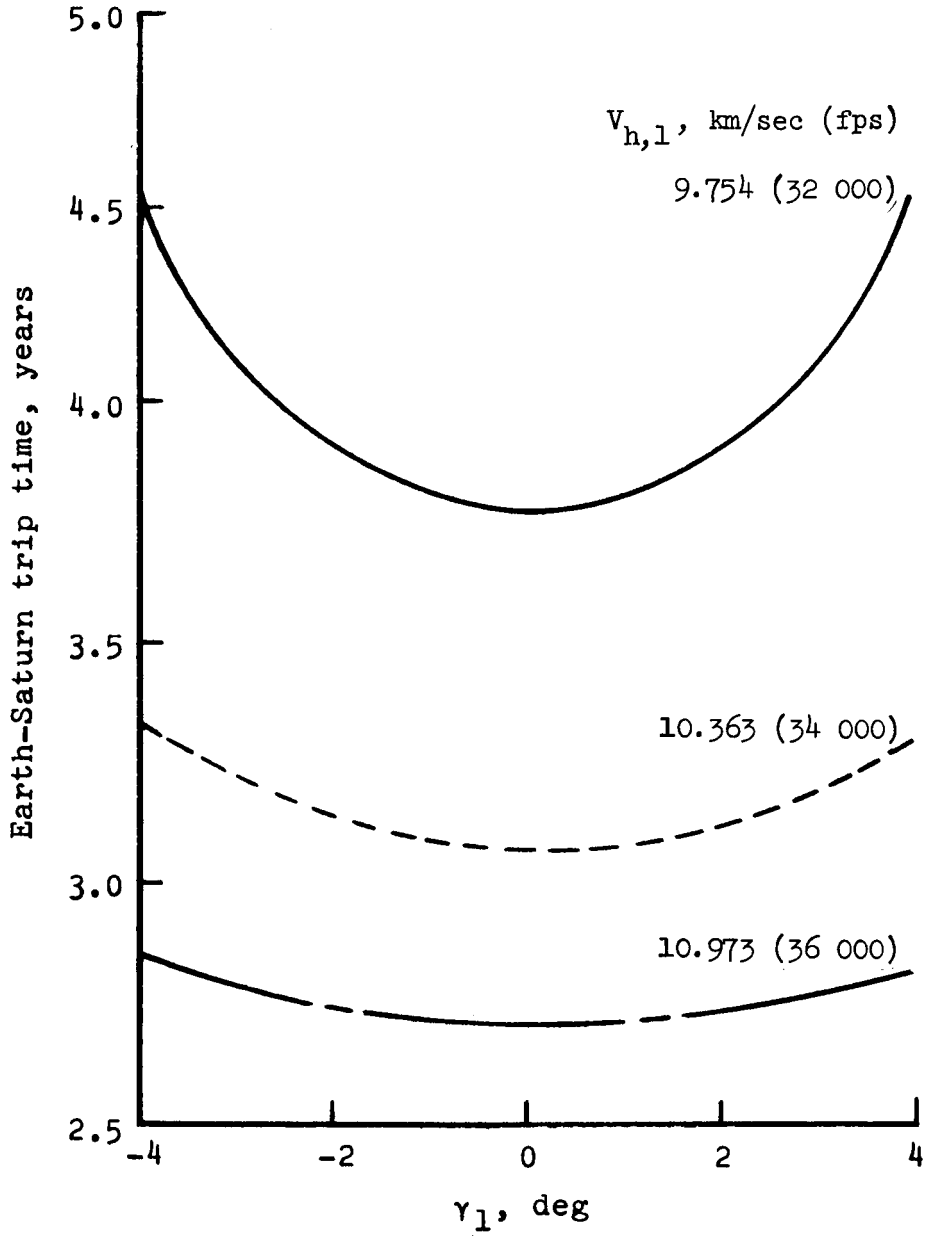

Figure 23.- Effect of hyperbolic-excess velocity and flight-path angle on trip time. Launch year, 1978.

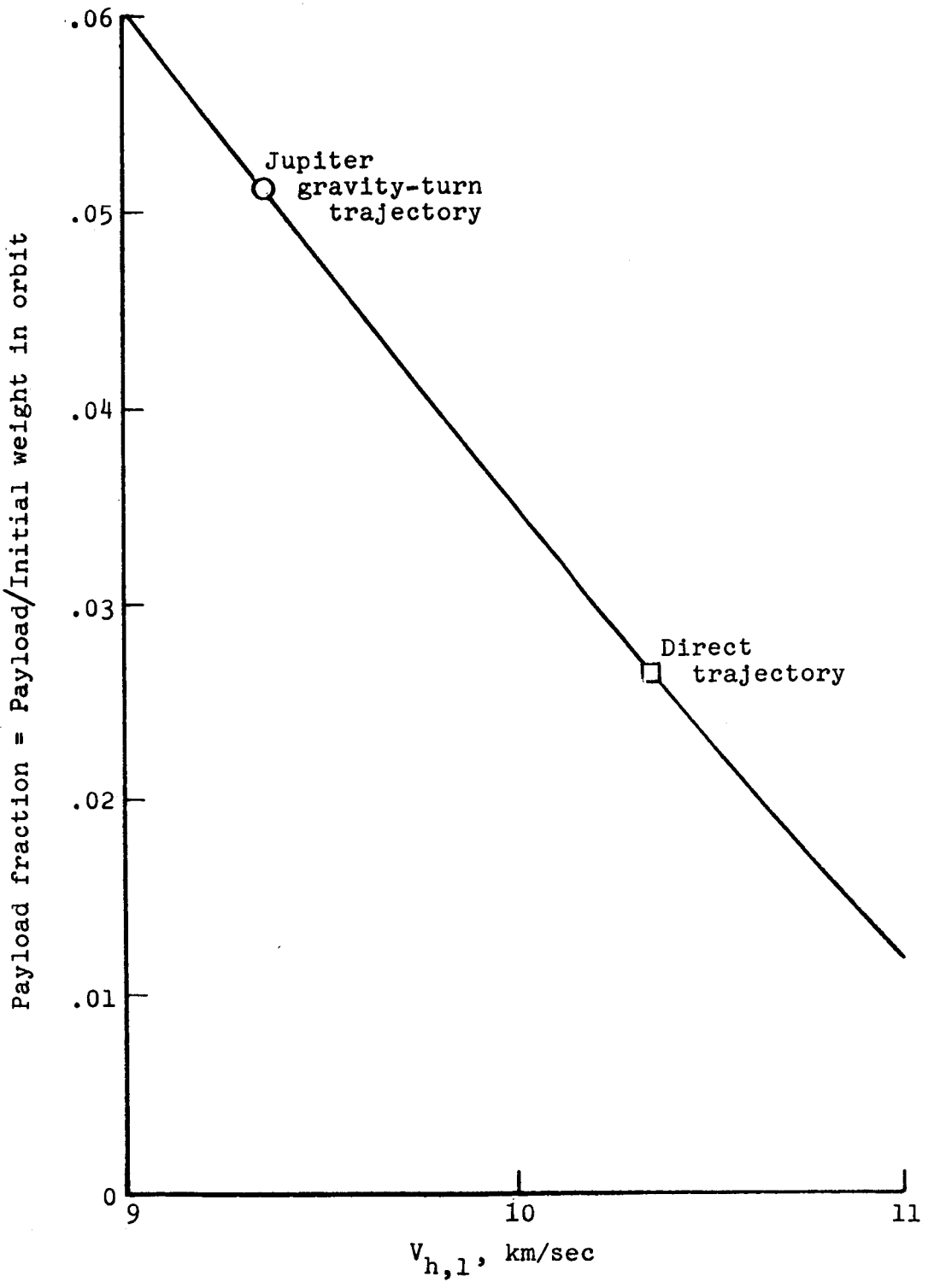

Figure 24.- Comparison of injected payload for a direct mission with a Jupiter gravity-turn mission to Saturn. I_{sp} = 4177.8 m/sec (426 lbf-sec/lbm); σ = 0.105.

"The aeronautical and space activities of the United States shall be conducted so as to contribute . . . to the expansion of human knowledge of phenomena in the atmosphere and space. The Administration shall provide for the widest practicable and appropriate dissemination of information concerning its activities and the results thereof."

—NATIONAL AERONAUTICS AND SPACE ACT OF 1958

NASA SCIENTIFIC AND TECHNICAL PUBLICATIONS

TECHNICAL REPORTS: Scientific and technical information considered important, complete, and a lasting contribution to existing knowledge.

TECHNICAL NOTES: Information less broad in scope but nevertheless of importance as a contribution to existing knowledge.

TECHNICAL MEMORANDUMS: Information receiving limited distribution because of preliminary data, security classification, or other reasons.

CONTRACTOR REPORTS: Technical information generated in connection with a NASA contract or grant and released under NASA auspices.

TECHNICAL TRANSLATIONS: Information published in a foreign language considered to merit NASA distribution in English.

TECHNICAL REPRINTS: Information derived from NASA activities and initially published in the form of journal articles.

SPECIAL PUBLICATIONS: Information derived from or of value to NASA activities but not necessarily reporting the results of individual NASA-programmed scientific efforts. Publications include conference proceedings, monographs, data compilations, handbooks, sourcebooks, and special bibliographies.

Details on the availability of these publications may be obtained from:

SCIENTIFIC AND TECHNICAL INFORMATION DIVISION

NATIONAL AERONAUTICS AND SPACE ADMINISTRATION

Washington, D.C. 20546